Calcolo (2024) 61:13
https://doi.org/10.1007/s10092-023-00563-z

Discontinuous Galerkin methods for Stokes equations under power law slip boundary condition: a priori analysis

Djoko Kamdem Jules[1] · **Gidey Hagos**[2] · **Koko Jonas**[3] · **Sayah Toni**[4]

Received: 25 June 2022 / Revised: 10 September 2023 / Accepted: 2 December 2023 /
Published online: 1 February 2024
© The Author(s) under exclusive licence to Istituto di Informatica e Telematica (IIT) 2024

Abstract

In this work, three discontinuous Galerkin (DG) methods are formulated and analysed to solve Stokes equations with power law slip boundary condition. Numerical examples exhibited confirm the theoretical findings, moreover we also test the methods on the lid Driven cavity and compare the three DG methods.

Keywords Power law · Anisotropic slip boundary condition · DG approximations · Error estimates · Rate of convergence

Mathematics Subject Classification 65N30 · 35J85

✉ Djoko Kamdem Jules
jules.djokokamdem@gmail.com

Gidey Hagos
gideyh@buist.ac.bw

Koko Jonas
jonas.koko@uca.fr

Sayah Toni
toni.sayah@usj.edu.lb

[1] School of Mathematical and Statistical Sciences, North West University, Potchefstroom, South Africa

[2] Department of Mathematics and Statistical Sciences, Botswana International University of Science and Technology, Palapye, Botswana

[3] LIMOS, Université Clermont-Auvergne – CNRS UMR 6158, B.P 10448, 63000 Clermont-Ferrand, France

[4] Laboratoire de Mathematiques et Applications, Unite de recherche "Mathematiques et Modelisation", Faculté des Sciences, Université Saint-Joseph, B.P 11-514, Riad El Solh, Beirut 1107 2050, Lebanon

1 Introduction

After a brief introduction in the modelling of Stokes equations with power law slip boundary condition, Sect. 1.2 is devoted to the a priori error estimates, which by the way constitute the main results of this work. These a priori error estimates are quasi optimal for some discontinuous Galerkin schemes, and independent of the power law parameter provided that the monotonicity is used with care.

1.1 Stokes equations with power law slip boundary condition

Let $\Omega \subset \mathbb{R}^d$, $d = 2, 3$ be a bounded domain occupied by a fluid with a boundary $\partial\Omega$. We are interested in the incompressible Stokes equations

$$-2\nu \operatorname{div} D\boldsymbol{u} + \nabla p = \boldsymbol{f} \quad \text{in } \Omega, \tag{1.1}$$

$$\operatorname{div} \boldsymbol{u} = 0 \quad \text{in } \Omega, \tag{1.2}$$

where ν is a positive parameter and represent the viscosity of the fluid. $\boldsymbol{u}(\boldsymbol{x})$ is the velocity, $p(\boldsymbol{x})$ is the pressure and $\boldsymbol{f}$ is the external force acting on the fluid. We recall that the Cauchy stress tensor is $\boldsymbol{T} = -p\boldsymbol{I} + 2\nu D\boldsymbol{u}$, with the symmetric part of the velocity gradient $2D\boldsymbol{u} = \nabla\boldsymbol{u} + (\nabla\boldsymbol{u})^T$. (1.1) and (1.2) are complemented by boundary conditions. Stokes and Navier–Stokes problems are most of the times analysed with Dirichlet type boundary conditions on the velocity field. But, in most situations such as oil ducts, water supply, microfluids channels or blood in arteries, different formulations with boundary conditions involving components of the velocity field, stress or pressure are of interest. A recent review of some of the formulations presented in the literature, and their associated boundary conditions, with a focus on applications to air and blood flows can be found in [20]. This work is the second part of the project started in [17] whose main aim is to analyse the numerical solution for flows with non-standard boundary conditions. The scope of the present work is to present discontinuous Galerkin (DG) schemes for Stokes system when the position and direction dependent slip boundary condition are taken into account. To describe the fluid on the boundary, we assume that $\partial\Omega$, the boundary of Ω, is partitioned into two disjoint components Γ_0 and Γ, with the measure of Γ_0 being positive. We assume that Γ_0 is the porous or artificial boundary where the fluid is prescribed, this is

$$\boldsymbol{u} = \boldsymbol{0} \quad \text{on } \Gamma_0\,. \tag{1.3}$$

On Γ, we assume the impermeability condition

$$\boldsymbol{u} \cdot \boldsymbol{n} = 0 \quad \text{on } \Gamma, \tag{1.4}$$

where $\boldsymbol{n} : S \longrightarrow \mathbb{R}^d$ is the normal outward unit vector to Γ. So, Γ is an impermeable solid surface along which the fluid may slip. In general for any vector $\boldsymbol{w}$ defined on $\partial\Omega$, we set $\boldsymbol{w}_{\boldsymbol{\tau}} = \boldsymbol{w} - (\boldsymbol{w} \cdot \boldsymbol{n})\boldsymbol{n}$. We note that $\boldsymbol{T}\boldsymbol{n}$ represents a vector field, that is the product of the matrix $\boldsymbol{T} = (T_{ij})$ and the vector $\boldsymbol{n} = (n_i)$. Hence, the tangential stress

$(\boldsymbol{Tn})_{\boldsymbol{\tau}}$ stands for the projection of the normal stress into the corresponding tangent plane. Taking the scalar product of $\boldsymbol{u}$ and (1.1), and using (1.2), (1.3) and (1.4), one has

$$2\nu \int_{\Omega} |D\boldsymbol{u}|^2 dx + \int_{\Gamma} (-\boldsymbol{Tn})_{\boldsymbol{\tau}} \cdot \boldsymbol{u}_{\boldsymbol{\tau}} d\sigma = \int_{\Omega} \boldsymbol{f} \cdot \boldsymbol{u} dx \tag{1.5}$$

with $d\sigma$ being the surface measure associated to Γ, and $\int_{\Gamma} (-\boldsymbol{Tn})_{\boldsymbol{\tau}} \cdot \boldsymbol{u}_{\boldsymbol{\tau}} d\sigma$ standing for dissipative processes on the Γ. So, it is clear that from (1.5), that one needs a functional relation between $(\boldsymbol{Tn})_{\boldsymbol{\tau}}$ and $\boldsymbol{u}_{\boldsymbol{\tau}}$. In this text, we consider the power law relation

$$(\boldsymbol{Tn})_{\boldsymbol{\tau}} + |K\boldsymbol{u}_{\boldsymbol{\tau}}|^{s-2} K^2 \boldsymbol{u}_{\boldsymbol{\tau}} = g \quad \text{on } \Gamma, \tag{1.6}$$

where $|\boldsymbol{v}|^2 = \boldsymbol{v} \cdot \boldsymbol{v}$ is the Euclidean norm and K is the anisotropic tensor, assumed to be uniformly positive definite, symmetric, $s \geq 1$ is a real number and g, the tangential surface traction. It is manifest from (1.5) that many choices of $(\boldsymbol{Tn})_{\boldsymbol{\tau}}$ and $\boldsymbol{u}_{\boldsymbol{\tau}}$ are possible. If $(\boldsymbol{Tn})_{\boldsymbol{\tau}} = \boldsymbol{0}$, then one gets a perfect slip boundary condition, while if $\boldsymbol{u}_{\boldsymbol{\tau}} = \boldsymbol{0}$, then there is no slip.

In [36, 37], the solvability of Stokes and Navier–Stokes are analyzed without (1.3) but (1.4) and (1.6) replaced by

$$\boldsymbol{u} \cdot \boldsymbol{n} = 0 \text{ and } \quad (\boldsymbol{Tn})_{\boldsymbol{\tau}} + H(\boldsymbol{u}_{\boldsymbol{\tau}})\boldsymbol{u}_{\boldsymbol{\tau}} = g \quad \text{on } \partial\Omega,$$

with $H(\boldsymbol{v}_{\boldsymbol{\tau}})$ behaving nicely. The situation in our hands is different. In fact for $s \neq 2$, the function $\boldsymbol{u} \longrightarrow \int_{\Gamma} |K\boldsymbol{u}_{\boldsymbol{\tau}}|^s d\sigma$ is not bounded below and above by the $L^2(\Gamma)$ norm of tangential component of the velocity. Hence the results obtained in [36, 37] do not cover the situation here. Thus in order to have a control on the velocity, we have divided the boundary $\partial\Omega$ into two parts, whereby on one part, Γ_0, we have imposed a Dirichlet boundary condition. This is a porous or artificial boundary where the fluid is prescribed. On the other part of the boundary, there is a functional relation between the tangential component of the traction and tangential part of the velocity.

The study of flows whose motion is described by Stokes or Navier Stokes equations driven by anisotropic slip boundary condition has been the subject of some publications recently (see [9–11, 29, 35–37, 39]). But it is worth mentioning that the numerical analysis of these problems it still lacking in the literature and one of the goals of this work is to start to develop numerical schemes for a better understanding of these phenomena. This work is a follow up of our first paper [17], where conforming finite element were presented. The aim in this contribution is to formulate, analyse and implement some DG schemes. The objective being to see how DG schemes will capture the nonlinear boundary condition, and how it will affect the convergence rate. At this juncture it is important to note that the power law we study here is completely different from the ones studied in [3, 26, 41], which is a result of the nonlinear representation of the Cauchy stress tensor. We also note that the power law boundary condition

formulated in [4, 6, 21, 31–34] is not direction dependent fluid model, but rather it is more appropriate to solid mechanics for bonded structures. Finally, we observe that (1.6) is a generalisation of the Navier's slip boundary condition, which is an active research direction (see [15, 16, 45–48] just to cite a few).

1.2 Main results

For conforming or non conforming finite element approximation, the Navier's slip relation on a part of the boundary leads in general to an a priori error estimate dominated by the interpolation error on the slip zone (see [15, 16, 45–48]). On the other side, for power law fluid, the a priori error estimate is also dominated by the power in the constitutive relation (see [3, 26, 41]). The problem (1.1), (1.2), (1.3), (1.4) and (1.6) is nonlinear and monotone type. Under mild regularity assumptions on the data g and $\boldsymbol{f}$, we have recently shown in [17] that it has a unique solution weak solution. We have also constructed a conforming finite element approximation and established its convergence. We propose to solve it now with a discretization that is locally mass conservative. The approximations of the velocity and pressure are discontinuous piecewise polynomials of different degrees. The discontinuous Galerkin methods used in this paper, encompasses the nonsymmetric interior penalty Galerkin (*NIPG*) method, the symmetric interior penalty Galerkin (*SIPG*) and the incomplete interior penalty Galerkin (*IIPG*) method introduced for elliptic problems in [1, 14, 40]. Several discontinuous Galerkin methods for elliptic problems are proposed and analysed in [2]. We establish the existence of solutions by means of Brouwer's fixed point, and show uniform convergence of the numerical method with respect to the parameter s by using a mesh dependent norm. It is worth noting that the convergence we get is optimal with respect to the mesh size and polynomial degree of the velocity. To be more precise, if $(\boldsymbol{u}, p)$ is the unique solution constructed in Theorem 2.1, and $(\boldsymbol{u}_h, p_h)$ is the DG solution constructed in Theorem 4.1, then

$$
\begin{aligned}
&|||\boldsymbol{u}-\boldsymbol{u}_h|||_h + \|\boldsymbol{u}_{\boldsymbol{\tau}} - \boldsymbol{u}_{\boldsymbol{\tau},h}\|_\Gamma + \|p-p_h\| \\
&\quad \le c\Big(\sum_{T\in\mathcal{T}_h} \|p-r_h p\|_T^2 + h_T^2\|\nabla(p-r_h p)\|_T^2\Big)^{1/2} + c|||\boldsymbol{u}-R_h\boldsymbol{u}|||_h \\
&\qquad + c\left(\sum_{e\in\mathcal{E}_h^\gamma} \|\boldsymbol{u}_{\boldsymbol{\tau}} - (R_h\boldsymbol{u})_{\boldsymbol{\tau}}\|_e\right)^{1/2},
\end{aligned}
$$

with r_h, R_h interpolation operators defined later, and $\mathcal{E}_h^\gamma$ the set of edges lying on slip zone, and $|||\cdot|||_h$ the mesh dependent norm. We note that the monotonicity of the nonlinear expression (1.6) is crucial in deriving a uniform a priori error estimate with respect to s. Those surprising results are in contrast with results obtained in [3, 26, 41] where the power in the constitutive relation is present in the error estimate (even though the power law in both situations are not the same). In this work, we do not study the case when $s > 2$, because the existence of the pressure is not clear to us even though the velocity can be constructed. The natural flexibility of the discontinuous

approximation spaces may allow the use of complicated geometries and unstructured meshes.

We propose a fixed point algorithm for solving the nonlinear system of equations generating by the discontinuous Galerkin approximation. The linearization of the nonlinear monotone term allow us to obtain a family of linear problem easy to solve. We prove that the fixed point algorithm has a unique solution, and most importantly, we show that this fixed point algorithm is convergent by using the weak convergence strategy inspired by [22, 38]. A similar fixed point strategy is proposed in [22] for solving steady Navier–Stokes equations. The reader can refer to the work of Glowinski [25] for a large variety of applications of such fixed-point approach. The final contribution of this work is about the verification of the theoretical results obtained. Indeed, in all examples discussed, it is manifest that both the *NIPG*, and *IIPG* methods perform better and unconditionally than the *SIPG* method. This conclusion was already predicted by the simple fact that the *SIPG* approach is conditionally well posed. This paper open the door for future applications of DG or non-conforming finite element schemes to monotone problems. The outline of the paper is as follows. Section 2 contains the preliminaries material for the mathematical formulation and understanding of the problem. The discontinuous Galerkin schemes are formulated in Sect. 3. The Existence of DG solutions are treated in Sect. 4, and Sect. 5 deals with the a priori error estimates of the DG schemes. In Sect. 6, we formulate and analyse the iterative scheme for solving the non linear finite element problem. We also implement the iterative scheme and exhibit some numerical results.

2 Known results

In this section, we introduce the notations that will be used throughout, recall the functional analysis framework needed to understand the concept of solutions of (1.1),(1.2),(1.3),(1.4) and (1.6), and summarise existing results related to this boundary value problem. We assume that $1 < s < 2$, and Ω is bounded open domain with a Lipschitz-continuous boundary $\partial\Omega$.

2.1 Notation

We adopt the standard definitions of Lebesgue and Sobolev spaces (see [8]). For $1 \leq p < \infty$

$$L^p(\Omega) = \left\{ v : \Omega \to \mathbb{R}; \quad v \text{ is measurable and } \int_\Omega |v(\boldsymbol{x})|^p d\boldsymbol{x} < \infty \right\},$$

with associated norm

$$\|v\|^p_{L^p(\Omega)} = \int_\Omega |v(\boldsymbol{x})|^p d\boldsymbol{x}$$

for which it is a Banach space, and for the special case $p = 2$, it is a Hilbert space with the norm that will be denoted by $\|\cdot\|$. Finally for $p = \infty$, one has

$$L^{\infty}(\Omega) = \left\{ v : \Omega \to \mathbb{R}, \quad \left| \begin{array}{r} v \text{ is measurable and there is a constant } c \\ \text{such that } |v(\boldsymbol{x})| \leq c \text{ a.e on } \Omega \end{array} \right. \right\},$$

with the associated norm

$$\|v\|_{L^{\infty}(\Omega)} = \|v\|_{\infty} = \inf\{c, \quad |v(\boldsymbol{x})| \leq c \text{ a.e on } \Omega\} .$$

Now, for any non-negative integer m and a real number $p \geq 1$, we defined the Sobolev space

$$W^{m,p}(\Omega) = \left\{ v \in L^p(\Omega), \quad \partial^{\alpha} v(\boldsymbol{x}) \in L^p(\Omega) \ \text{ for all } |\alpha| \leq m \right\},$$

with $\alpha = (\alpha_1, \ldots, \alpha_d)$ the multi-index with $|\alpha| = \alpha_1 + \cdots + \alpha_d$, and $\partial^{\alpha} v(\boldsymbol{x})$ the distributional derivative of v given by

$$\partial^{\alpha} v = \frac{\partial^{|\alpha|} v}{\partial x_1^{\alpha_1} \cdots \partial x_d^{\alpha_d}}.$$

The space $W^{m,p}(\Omega)$ is equipped with the semi-norm and norm

$$|v|^p_{W^{m,p}(\Omega)} = \sum_{|\alpha|=m} \int_{\Omega} \left|\partial^{\alpha} v(\boldsymbol{x})\right|^p d\boldsymbol{x} , \quad \|v\|^p_{m,p} = \sum_{0 \leq |\alpha| \leq m} \int_{\Omega} \left|\partial^{\alpha} v(\boldsymbol{x})\right|^p d\boldsymbol{x}.$$

Throughout the paper, boldface characters denote vector quantities, etc.
We note that $W^{m,2}(\Omega) = H^m(\Omega)$ and $H^0(\Omega)$ coincides with $L^2(\Omega)$, for which the norm and inner product are denoted as $\|\cdot\|$ and $(\cdot, \cdot)$, respectively.
Since $1 < s < 2$, we have $\|\boldsymbol{u}_{\boldsymbol{\tau}}\|_{L^1(\Gamma)} \leq c\|\boldsymbol{u}_{\boldsymbol{\tau}}\|_{L^s(\Gamma)} \leq c\|\boldsymbol{u}_{\boldsymbol{\tau}}\|_{L^2(\Gamma)}$. Hence the velocity is prescribed in

$$\mathbb{V} = \left\{ \boldsymbol{v} \in H^1(\Omega)^d : \ \text{ with } \ \boldsymbol{v}|_{\Gamma_0} = 0 \text{ and } \boldsymbol{v} \cdot \boldsymbol{n}|_{\Gamma} = 0 \right\},$$

equipped with the regular $\boldsymbol{H}^1$-norm, while the pressure is in the space

$$M = \left\{ p \in L^2(\Omega) : \quad (p, 1) = 0 \right\} = L^2_0(\Omega).$$

It is worth mentioning that the zero mean value is added on the pressure to avoid the pressure given in (1.1) or (1.6), and (1.2) to be determined up to a constant. It should be noted that the spaces $\mathbb{V}$ and M are compatible in the sense that; there exists β such that (see [5, 22])

$$\text{for all } p \in M, \quad \beta\|p\| \leq \sup_{\boldsymbol{v} \in \mathbb{V}} \frac{(p, \operatorname{div} \boldsymbol{v})}{\|\boldsymbol{v}\|_1}. \tag{2.1}$$

Remark 2.1 When $2 < s$, we have $\|\boldsymbol{u_\tau}\|_{L^2(\Gamma)} \leq c\|\boldsymbol{u_\tau}\|_{L^s(\Gamma)}$. Then the velocity is prescribed in

$$\mathbb{V} = \left\{ \boldsymbol{v} \in H^1(\Omega)^d \ , \ \boldsymbol{v_\tau} \in L^s(\Gamma)^d \ : \ \text{with} \ \ \boldsymbol{v}|_{\Gamma_0} = 0 \ \text{and} \ \boldsymbol{v} \cdot \boldsymbol{n}|_\Gamma = 0 \right\}$$

equipped with the norm

$$|||\boldsymbol{v}|||^2 = \|\boldsymbol{v}\|_1^2 + \|\boldsymbol{v_\tau}\|_{L^s(\Gamma)}^2 \ .$$

The pressure is prescribed in the same function space $M = L_0^2(\Omega)$, but the difficulty in this situation is to prove (2.1).

2.2 Variational analysis

We assume that $(\boldsymbol{f}, g) \in \boldsymbol{L}^2(\Omega) \times L^\infty(\Gamma)$, and consider the following variational formulation for problem (1.1),(1.2),(1.3),(1.4) and (1.6)

$$\begin{cases} \text{Find } (\boldsymbol{u}, p) \in \mathbb{V} \times M \text{ such that for all } (\boldsymbol{v}, q) \in \mathbb{V} \times M, \\ a(\boldsymbol{u}, \boldsymbol{v}) + \displaystyle\int_\Gamma |K\boldsymbol{u_\tau}|^{s-2} K\boldsymbol{u_\tau} \cdot K\boldsymbol{v_\tau} d\sigma - b(\boldsymbol{v}, p) = \ell(\boldsymbol{v}), \\ b(\boldsymbol{u}, q) = 0, \end{cases} \tag{2.2}$$

with $a(\boldsymbol{u}, \boldsymbol{v}) = 2\nu \displaystyle\int_\Omega D\boldsymbol{u} : D\boldsymbol{v} d\boldsymbol{x}$, $b(\boldsymbol{v}, q) = \displaystyle\int_\Omega q \, \mathrm{div}\, \boldsymbol{v} d\boldsymbol{x}$, $\ell(\boldsymbol{v}) = \displaystyle\int_\Omega \boldsymbol{f} \cdot \boldsymbol{v} d\boldsymbol{x} + \int_\Gamma g \boldsymbol{v_\tau} d\sigma$, and $\boldsymbol{A} : \boldsymbol{B} = \sum_{1 \leq i,j \leq d} A_{ij} B_{ij}$. We recall that the identity $\sum_{1 \leq i,j \leq d} D_{ij}\boldsymbol{u} \dfrac{\partial v_i}{\partial x_j} = \sum_{1 \leq i,j \leq d} D_{ij}\boldsymbol{u} D_{ij}\boldsymbol{v}$ which is the consequence of the symmetry of $D\boldsymbol{u}$.

Remark 2.2 In many contributions, the conservation of the momentum is expressed in terms of the Laplacian of the velocity which gives rise to the bilinear form $\widetilde{a}(\boldsymbol{u}, \boldsymbol{v}) = 2\nu \displaystyle\int_\Omega \nabla \boldsymbol{v} : \nabla \boldsymbol{u} dx$, instead of $a(\cdot, \cdot)$ defined before. Although at a continuous level

$$\mathrm{div}\, \boldsymbol{u} = 0 \quad \text{implies that} \quad \mathrm{div}\, D\boldsymbol{u} = \Delta \boldsymbol{u},$$

from a modeling viewpoint it may be important to work with symmetric tensor $D\boldsymbol{u}$. For instance, the problem (1.1)–(1.6) gives directly the natural boundary condition in term of the force exerted by the fluid (the traction force $\boldsymbol{T}(\boldsymbol{u}, p)\boldsymbol{n}$) on the boundary Γ.

The usual standard arguments leads to the following result

Proposition 2.1 *Any couple* $(\boldsymbol{u}, p) \in \mathbb{V} \times M$ *is a solution of* (1.1), (1.2), (1.3), (1.4) *and* (1.6) *(in the sense of distribution) if and only if it is a solution of* (2.2).

To study (2.2) it is convenient to recall the following monotonicity and continuity properties (see [26, 41]): there exists a constant c independent of $\boldsymbol{x}$, $\boldsymbol{y}$ such that for $1 \leq s < 2$

$$(|\boldsymbol{y}| + |\boldsymbol{x}|)^{2-s} \left(|\boldsymbol{y}|^{s-2}\boldsymbol{y} - |\boldsymbol{x}|^{s-2}\boldsymbol{x}, \boldsymbol{y} - \boldsymbol{x} \right) \geq c|\boldsymbol{x} - \boldsymbol{y}|^2 \quad \text{for all } \boldsymbol{x}, \boldsymbol{y} \in \mathbb{R}^n, \tag{2.3}$$

and

$$\left| |\boldsymbol{x}|^{s-2}\boldsymbol{x} - |\boldsymbol{y}|^{s-2}\boldsymbol{y} \right| \leq c|\boldsymbol{x} - \boldsymbol{y}|^{s-1} \text{ for all } \boldsymbol{x}, \boldsymbol{y} \in \mathbb{R}^d. \tag{2.4}$$

Now we introduce the mapping $\boldsymbol{v} \longrightarrow \mathcal{A}(\boldsymbol{v})$ defined as follows

$$\text{for all } \boldsymbol{w} \in \mathbb{V}_{\text{div}}\ ,\ \mathcal{A}(\boldsymbol{v})\boldsymbol{w} = \int_\Gamma |K\boldsymbol{v}_{\boldsymbol{\tau}}|^{s-2} K\boldsymbol{v}_{\boldsymbol{\tau}} \cdot K\boldsymbol{w}_{\boldsymbol{\tau}} d\sigma. \tag{2.5}$$

We claim that

Lemma 2.1 *(a) $\mathcal{A}$ maps $\mathbb{V}_{\text{div}}$ into its dual $\mathbb{V}'_{\text{div}}$, and is bounded on all bounded subsets of $\mathbb{V}_{\text{div}}$.*

(b) For all $\boldsymbol{v}, \boldsymbol{u}$ elements of $\mathbb{V}_{\text{div}}$, $\|\mathcal{A}(\boldsymbol{v}) - \mathcal{A}(\boldsymbol{u})\|_{\mathbb{V}'} \leq c\|K\|^s_{L^\infty(\Gamma)} \|\boldsymbol{u} - \boldsymbol{v}\|_1^{s-1}$.

Proof These properties are obtained by using; Hölder's and Cauchy–Schwarz's inequalities and (2.4). □

The solution of (2.2) is constructed by using the theory of monotone operator. We recall that (2.2) is equivalent to (see [22, 38])

$$\begin{cases} \text{Find } \boldsymbol{u} \in \mathbb{V}_{\text{div}} \text{ such that for all } \boldsymbol{v} \in \mathbb{V}_{\text{div}}, \\ a(\boldsymbol{u}, \boldsymbol{v}) + \displaystyle\int_\Gamma |K\boldsymbol{u}_{\boldsymbol{\tau}}|^{s-2} K\boldsymbol{u}_{\boldsymbol{\tau}} \cdot K\boldsymbol{v}_{\boldsymbol{\tau}} d\sigma = \ell(\boldsymbol{v}). \end{cases} \tag{2.6}$$

Owing to that equivalence, we restrict the analysis to problem (2.6). We shall prove that the left hand side of (2.6) is strictly monotone, coercive and hemi-continuous in $\mathbb{V}$. Then the existence and uniqueness of (2.6) will follow by standard arguments, see [38, Chap 2]. First we claim that

Proposition 2.2 [17] *(a) The mapping $\boldsymbol{v} \to \mathcal{A}\boldsymbol{v}$ defined by (2.5) is strictly monotone from $\mathbb{V}$ into $\mathbb{V}'_{\text{div}}$:*

$$\textit{For all } \boldsymbol{v}, \boldsymbol{w} \in \mathbb{V}_{\text{div}}, \quad (\mathcal{A}\boldsymbol{v} - \mathcal{A}\boldsymbol{w})(\boldsymbol{v} - \boldsymbol{w}) > 0\ .$$

(b) $\mathcal{A}$ is hemi-continuous in $\mathbb{V}_{\text{div}}$, this is to say that for $\boldsymbol{u}, \boldsymbol{v}$ in $\mathbb{V}_{\text{div}}$, the mapping $t \longrightarrow \mathcal{A}(\boldsymbol{u} + t\boldsymbol{v})\boldsymbol{v}$ is continuous from $\mathbb{R}$ into $\mathbb{R}$.

(c) $\mathcal{A}$ is coercive, i.e $\displaystyle\lim_{\|\boldsymbol{v}\|_1 \to \infty} \frac{1}{\|\boldsymbol{v}\|_1} (a(\boldsymbol{v}, \boldsymbol{v}) + \mathcal{A}(\boldsymbol{v})\boldsymbol{v}) = \infty.$

From Proposition 2.2, we deduce that

Theorem 2.1 *If $1 < s < 2$, then the variational problem (2.2) has a unique solution $(\boldsymbol{u}, p) \in \mathbb{V} \times M$, which moreover satisfy the bounds*

$$\nu c\|\nabla \boldsymbol{u}\|^2 + \int_\Gamma |K\boldsymbol{u}_\tau|^s \, d\sigma \le c\|\boldsymbol{f}\|^2 + c\|g\|^2_{L^\infty(\Gamma)},$$

and

$$\|p\| \le 2\nu\|\nabla \boldsymbol{u}\| + \|K\|^s_{L^\infty(\Gamma)} \|\boldsymbol{u}_\tau\|^{s-1}_{L^s(\Gamma)} + c\|\boldsymbol{f}\| + c\|g\|_{L^\infty(\Gamma)}.$$

3 Finite element approximations

In this text, we intend to develop discontinuous Galerkin finite approximations for the numerical solution of (2.2).

3.1 Notation and approximation properties

We assume that Ω is a polygonal domain of $\mathbb{R}^2$. Let $\mathcal{T} = \{T\}$ be a regular family of triangulation of $\overline{\Omega}$, consisting of triangles of maximum diameter h. Let h_T be a diameter of a triangle T and ρ_T the diameter of its inscribed circle. With abuse of notation we denote the triangulation $\mathcal{T}_h$ instead of $\mathcal{T}$. By regular we mean that there exists a parameter $\sigma > 0$ such that

$$\text{for all } K \in \mathcal{T}_h, \quad \frac{h_T}{\rho_T} = \sigma_T \le \sigma. \tag{3.1}$$

If e is a face of $T \in \mathcal{T}_h$, then h_e is the length of e. Let $\mathcal{E}_h = \{e\}$ denote the set of the edges of $\mathcal{T}_h$, and $\mathcal{E}_h^0 = \mathcal{E}_h \backslash \overline{\Gamma}$ the set of all edges not lying on $\overline{\Gamma}$, and $\mathcal{E}_h^\gamma$ the set of all edges lying on $\overline{\Gamma}$. $\mathcal{E}_h^I$ is the set of all interior edges. We associate with each edge of an element K_i, the outward unit normal vector $\boldsymbol{n}_i$. For an edge that lies on the boundary, $\boldsymbol{n}_i$ is defined to be the outward normal to $\partial\Omega$. For a positive integer m, we set

$$H^m(\mathcal{T}_h) = \left\{ v \in L^2(\Omega), \quad v|_T \in H^m(T), \quad \text{for all } T \in \mathcal{T}_h \right\},$$
$$T(\mathcal{E}_h) = \prod_{T \in \mathcal{T}_h} L^2(\partial T).$$

In this work, for each edge e, we associate a normal unit vector $\boldsymbol{n}$. If the e is on the boundary, the unit vector $\boldsymbol{n}$ is taken to be the outward normal to $\partial\Omega$. Let e_k be an edge shared by elements T_i and T_j with $\boldsymbol{n}_k$ exterior to T_i. We define the jump $[v]_k$ and average $\{v\}_k$ of a function v by

$$[v]_k = v|_{\partial T_i} - v|_{\partial T_j}, \quad \{v\}_k = \frac{1}{2}\left(v|_{\partial T_i} + v|_{\partial T_j}\right).$$

If $e = T_i \cap \partial\Omega$, then the jumps and average of v coincide with its trace on e.

The following identity obtained by re-arranging terms relates the scalar product of two quantities to the products of their jumps and averages

$$\begin{aligned}\sum_{T\in\mathcal{T}_h}\int_{\partial T}\boldsymbol{v}\cdot\boldsymbol{T}\boldsymbol{n}d\sigma &= \sum_{e\in\mathcal{E}_h}\int_e[\boldsymbol{v}]\cdot\{\boldsymbol{T}\}\boldsymbol{n}_e d\sigma+\sum_{e\in\mathcal{E}_h^I}\int_e\{\boldsymbol{v}\}\cdot[\boldsymbol{T}]\boldsymbol{n}_e d\sigma,\\ \sum_{T\in\mathcal{T}_h}\int_{\partial T}q\boldsymbol{v}\cdot\boldsymbol{n}d\sigma &= \sum_{e\in\mathcal{E}_h}\int_e[\boldsymbol{v}]\cdot\boldsymbol{n}_e\{q\}d\sigma+\sum_{e\in\mathcal{E}_h^I}\int_e\{\boldsymbol{v}\}\cdot\boldsymbol{n}_e[q]d\sigma.\end{aligned}\tag{3.2}$$

The velocity and pressure will be approximated by $\mathbb{V}_h$ and M_h given as follows

$$\begin{aligned}\widetilde{\mathbb{V}}_h &= \left\{\boldsymbol{v}\in\boldsymbol{L}^2(\Omega):\quad \boldsymbol{v}|_T\in\mathcal{P}_k(T)^2 \text{ for all } T\in\mathcal{T}_h\right\},\\ \mathbb{V}_h &= \left\{\boldsymbol{v}\in\boldsymbol{L}^2(\Omega):\quad \boldsymbol{v}|_T\in\mathcal{P}_k(T)^2 \text{ for all } T\in\mathcal{T}_h,\ \text{and}\ \boldsymbol{v}\cdot\boldsymbol{n}_e=0 \text{ for all } e\in\mathcal{E}_h^\gamma\right\},\\ M_h &= \left\{q\in L_0^2(\Omega):\quad q|_T\in\mathcal{P}_{k-1}(T)\ \text{ for all } T\in\mathcal{T}_h\right\},\end{aligned}$$

with $\mathcal{P}_k(T)$ the space of polynomials for degree at most k in $T\in\mathcal{T}_h$. In the sequel, we denote by $c, c', \ldots$ generic constants that can vary from line to line but are always independent of all discretization parameter. Having in mind that $\mathcal{T}_h$ is regular (see (3.1)), for each $k\geq 1$, one can construct an operator $r_h\in\mathcal{L}(L_0^2(\Omega);M_h)$ such that

$$\begin{cases}\text{for any } T\in\mathcal{T}_h \text{ and for all } (q,p)\in\mathcal{P}_{k-1}(T)\times L_0^2(\Omega),\\ \displaystyle\int_T q\,(r_h p-p)\,d\boldsymbol{x}=0,\end{cases}$$

moreover

$$\begin{cases}\text{for any real } s\in[0,k] \text{ and for all } q\in H^s(\Omega)\cap L_0^2(\Omega)\\ \|r_h q-q\|_T\leq c h_T^s|q|_{s,T},\end{cases}\tag{3.3}$$

with $|\cdot|_{s,T}$ the semi-norm. The interpolation of functions belonging to $\mathbb{V}_h$ is a bit delicate because the normal component of the velocity must be zero for all edges $e\in\mathcal{E}_h^\gamma$. So, we consider the interpolation operator of Raviart–Thomas [22, 42] $\Pi\in\mathcal{L}(H^1(\Omega)^2;\widetilde{\mathbb{V}}_h)$ satisfying the following properties:

$$\begin{aligned}&\forall(\boldsymbol{v},T,q_h)\in H^1(\Omega)^2\times\mathcal{T}_h\times\mathcal{P}_{k-1}(T),\ \int_T q_h\,\mathrm{div}(\Pi\boldsymbol{v}-\boldsymbol{v})dx=0,\\ &\forall(\boldsymbol{v},e,q_h)\in H^1(\Omega)^2\times\mathcal{E}_h^0\times\mathcal{P}_{k-1}(e),\ \int_e q_h(\Pi\boldsymbol{v}-\boldsymbol{v})\cdot\boldsymbol{n}_e d\sigma=0,\\ &\forall\boldsymbol{v}\in H^1(\Omega)^2,\ |||\Pi\boldsymbol{v}|||_h\leq c\|\nabla\boldsymbol{v}\|,\\ &\forall(\boldsymbol{v},T)\in H^1(\Omega)^2\times\mathcal{T}_h,\ \|\nabla(\boldsymbol{v}-\Pi\boldsymbol{v})\|_T+\frac{1}{h_T}\|\boldsymbol{v}-\Pi\boldsymbol{v}\|_T\leq c\|\nabla\boldsymbol{v}\|_T.\end{aligned}\tag{3.4}$$

3.2 Discontinuous Galerkin approximations

In this paragraph, we present DG schemes for solving the mixed variational problem (2.2). These methods can be found in [1, 2, 14, 40]. For any $\boldsymbol{v}_h \in \mathbb{V}_h$, we define $\nabla_h \boldsymbol{v}_h$, $\mathrm{div}_h\, \boldsymbol{v}_h$, $D_h(\boldsymbol{v}_h)$ and $\boldsymbol{T}_h(\boldsymbol{v}_h)$ as follows: for any $T \in \mathcal{T}_h$

$$\begin{aligned} &\nabla_h \boldsymbol{v}_h = \nabla \boldsymbol{v}_h, \quad \mathrm{div}_h\, \boldsymbol{v}_h = \mathrm{div}\, \boldsymbol{v}_h \\ &D_h \boldsymbol{v}_h = D\boldsymbol{v}_h, \quad \boldsymbol{T}_h(\boldsymbol{v}_h) = 2\nu D_h \boldsymbol{v}_h - p_h \boldsymbol{I} \quad . \end{aligned}$$

In this text, we will consider three formulations. The bilinear forms of the first two formulations are defined as follows

$$\begin{aligned} A(\boldsymbol{v}, \boldsymbol{w}) = 2\nu \sum_{T\in\mathcal{T}_h} \int_T D\boldsymbol{v} : D\boldsymbol{w} d\boldsymbol{x} - 2\nu \sum_{e\in\mathcal{E}_h^0} \int_e \Big(\{D\boldsymbol{v}\}\boldsymbol{n}_e \cdot [\boldsymbol{w}] - \epsilon_0 \{D\boldsymbol{w}\}\boldsymbol{n}_e \cdot [\boldsymbol{v}] \Big) d\sigma \\ + \sum_{e\in\mathcal{E}_h^0} \int_e \frac{\alpha}{h_e} [\boldsymbol{v}] \cdot [\boldsymbol{w}] d\sigma, \\ B(\boldsymbol{v}, q) = -\sum_{T\in\mathcal{T}_h} \int_T q\, \mathrm{div}\, \boldsymbol{v} d\boldsymbol{x} + \sum_{e\in\mathcal{E}_h^0} \int_e \{q\} [\boldsymbol{v}] \cdot \boldsymbol{n}_e d\sigma, \end{aligned} \tag{3.5}$$

where we take the constant value $\epsilon_0 = \{-1, 0, 1\}$, and α is the jump parameter that will be made precise later. In what follows, $A(\cdot, \cdot)$ can be one of the three bilinear forms given in (3.5). In addition to the bilinear form $A(\cdot, \cdot)$, one considers the following linear and bilinear forms

$$\begin{aligned} F(\boldsymbol{v}) &= \sum_{T\in\mathcal{T}_h} \int_T \boldsymbol{f} \cdot \boldsymbol{v} dx + \sum_{e\in\mathcal{E}_h^\gamma} \int_e g \boldsymbol{v}_{\boldsymbol{\tau}} d\sigma, \\ H(\boldsymbol{v})\boldsymbol{w} &= \sum_{e\in\mathcal{E}_h^\gamma} \int_e |K\boldsymbol{v}_{\boldsymbol{\tau}}|^{s-2} K\boldsymbol{v}_{\boldsymbol{\tau}} \cdot K\boldsymbol{w}_{\boldsymbol{\tau}} d\sigma. \end{aligned}$$

Finally, we consider the following DG-method:

$$\begin{cases} \text{Find } (\boldsymbol{u}_h, p_h) \in \mathbb{V}_h \times M_h, \text{ such that for all } (\boldsymbol{v}_h, q_h) \in \mathbb{V}_h \times M_h, \\ A(\boldsymbol{u}_h, \boldsymbol{v}_h) + B(\boldsymbol{v}_h, p_h) + H(\boldsymbol{u}_h)\boldsymbol{v}_h = F(\boldsymbol{v}_h), \\ B(\boldsymbol{u}_h, q_h) = 0. \end{cases} \tag{3.6}$$

Remark 3.1 When $\epsilon_0 = -1$, we note that $A(\boldsymbol{v}, \boldsymbol{w}) = A(\boldsymbol{w}, \boldsymbol{v})$, and we let $A(\cdot, \cdot) = A^{SIPG}(\cdot, \cdot)$. So the scheme (3.6) is called the symmetric interior penalty Galerkin scheme *SIPG* (see [1]). For $\epsilon_0 = 1$, the method (3.6) is called the non-symmetric interior penalty Galerkin scheme *NIPG* (see [40]), and we let $A(\cdot, \cdot) = A^{NIPG}(\cdot, \cdot)$, and for $\epsilon = 0$, the scheme (3.6) is the incomplete interior penalty Galerkin scheme *IIPG* introduced by Dawson, Sun and Wheeler for elliptic problems in [14].

We associate with $\mathbb{V}_h$ the norm,

$$|||\boldsymbol{v}|||_h^2 = \sum_{T\in\mathcal{T}_h} \|D\boldsymbol{v}\|_T^2 + \sum_{e\in\mathcal{E}_h^0} \frac{1}{h_e}\|[\boldsymbol{v}]\|_e^2 \quad \text{for all } \boldsymbol{v}\in\mathbb{V}_h.$$

Remark 3.2 Note that, by using Korn's type inequality (see [7]), for any $\boldsymbol{v}_h \in \mathbb{V}_h$ we get

$$\sum_{T\in\mathcal{T}_h} \|\nabla \boldsymbol{v}_h\|_T^2 \leq c\Big(\sum_{T\in\mathcal{T}_h} \|D\boldsymbol{v}_h\|_T^2 + \sum_{e\in\mathcal{E}_h^0} \frac{1}{h_e}\|[\boldsymbol{v}_h]\|_e^2\Big).$$

Thus on $\mathbb{V}_h$, $|||\cdot|||_h$ is equivalent to the norm

$$\boldsymbol{v}_h \longrightarrow \Big(\sum_{T\in\mathcal{T}_h} \|\nabla \boldsymbol{v}_h\|_T^2 + \sum_{e\in\mathcal{E}_h^0} \frac{1}{h_e}\|[\boldsymbol{v}_h]\|_e^2\Big)^{1/2}.$$

The bilinear forms $A(\cdot,\cdot)$ and $B(\cdot,\cdot)$ given in (3.5) can be written as follows

$$\begin{aligned} A(\boldsymbol{v}_h, \boldsymbol{w}_h) &= a(\boldsymbol{v}_h, \boldsymbol{w}_h) + s(\boldsymbol{v}_h, \boldsymbol{w}_h),\\ B(\boldsymbol{v}_h, q_h) &= b(\boldsymbol{v}_h, q_h) + \sum_{e\in\mathcal{E}_h^0} \int_e \{q\}[\boldsymbol{v}]\cdot \boldsymbol{n}_e d\sigma, \end{aligned} \tag{3.7}$$

with

$$s(\boldsymbol{v},\boldsymbol{w}) = -2\nu \sum_{e\in\mathcal{E}_h^0} \int_e \Big(\{D\boldsymbol{v}\}\boldsymbol{n}_e\cdot[\boldsymbol{w}] - \epsilon_0\{D\boldsymbol{w}\}\boldsymbol{n}_e\cdot[\boldsymbol{v}]\Big)d\sigma + \sum_{e\in\mathcal{E}_h^0}\int_e \frac{\alpha}{h_e}[\boldsymbol{v}]\cdot[\boldsymbol{w}]d\sigma.$$

With (3.2) in mind, we have that

Lemma 3.1 (consistency) *Let $(\boldsymbol{u}, p)$ be the solution of (2.2) with $(\boldsymbol{u}, p) \in H^2(\Omega)^2 \times H^1(\Omega)$, then*

$$\begin{cases} \text{for all } (\boldsymbol{v}_h, q_h) \in \mathbb{V}_h \times M_h,\\ A(\boldsymbol{u}, \boldsymbol{v}_h) + B(\boldsymbol{v}, p) + H(\boldsymbol{u})\boldsymbol{v}_h = F(\boldsymbol{v}_h),\\ B(\boldsymbol{u}, q_h) = 0. \end{cases}$$

Proof Let $q_h \in M_h$, from the regularity assumption $\boldsymbol{u} \in H^2(\Omega)^2$, we deduce that (1.2) holds pointwise. Thus, we multiply it by $q_h \in M_h$, and integrate over Ω to obtain

$$b(\boldsymbol{u}, q_h) = 0.$$

But we have (see (3.7))

$$B(\boldsymbol{u}, q_h) = b(\boldsymbol{u}, q_h) + \sum_{e\in\mathcal{E}_h^0}\int_e \{q_h\}[\boldsymbol{u}]\cdot\boldsymbol{n}_e d\sigma = \sum_{e\in\mathcal{E}_h^0}\int_e \{q_h\}[\boldsymbol{u}]\cdot\boldsymbol{n}_e d\sigma.$$

Since $\boldsymbol{u}\in H^2(\Omega)^2$, we have $\boldsymbol{u}\in H^1_{loc}(\Omega)^2$. We use a result due to Evans and Gariepy (see [18, Section 4.9.2, Theorem 2]), according to which functions in $H^1_{loc}(\Omega)$ are continuous across interior edges in Ω. Thus jumps terms involving $\boldsymbol{u}$ is zero. Thus

$$B(\boldsymbol{u}, q_h) = 0.$$

Next, for $\boldsymbol{v}_h\in\mathbb{V}_h\times M_h$, from the regularity assumption $(\boldsymbol{u}, p)\in H^2(\Omega)^2\times H^1(\Omega)$, we deduce that (1.1) holds pointwise. We multiply the (1.1) by $\boldsymbol{v}_h$, integrating by parts on $K\in\mathcal{T}_h$, and using (3.2), we obtain

$$\begin{aligned}
&2\nu\sum_{T\in\mathcal{T}_h}\int_T D\boldsymbol{u} : D\boldsymbol{v}_h dx - \sum_{T\in\mathcal{T}_h}\int_T p\,\mathrm{div}\,\boldsymbol{v}_h dx - 2\nu\sum_{e\in\mathcal{E}_h^I}\int_e [D\boldsymbol{u}]\boldsymbol{n}_e : \{\boldsymbol{v}_h\}d\sigma\\
&\quad - 2\nu\sum_{e\in\mathcal{E}_h}\int_e \{D\boldsymbol{u}\}\boldsymbol{n}_e : [\boldsymbol{v}_h]d\sigma + \sum_{e\in\mathcal{E}_h^I}\int_e [p]\boldsymbol{n}_e\cdot\{\boldsymbol{v}_h\}d\sigma + \sum_{e\in\mathcal{E}_h}\int_e \{p\}\boldsymbol{n}_e\cdot[\boldsymbol{v}_h]d\sigma\\
&= \sum_{T\in\mathcal{T}_h}\int_T \boldsymbol{f}\cdot\boldsymbol{v}_h dx.
\end{aligned} \tag{3.8}$$

Since $\boldsymbol{u}\in H^2(\Omega)^2$, we have $D\boldsymbol{u}\in H^1(\Omega)^{2\times 2}$ and hence in $H^1_{loc}(\Omega)^{2\times 2}$. Thus from Evans and Gariepy (see [18, Section 4.9.2, Theorem 2]), the jumps terms involving $D\boldsymbol{u}$ and p vanish. Thus (3.8) gives

$$\begin{aligned}
&2\nu\sum_{T\in\mathcal{T}_h}\int_T D\boldsymbol{u} : D\boldsymbol{v}_h dx - \sum_{T\in\mathcal{T}_h}\int_T p\,\mathrm{div}\,\boldsymbol{v}_h dx - 2\nu\sum_{e\in\mathcal{E}_h}\int_e \{D\boldsymbol{u}\}\boldsymbol{n}_e : [\boldsymbol{v}_h]d\sigma\\
&\quad + \sum_{e\in\mathcal{E}_h}\int_e \{p\}\boldsymbol{n}_e\cdot[\boldsymbol{v}_h]d\sigma = \sum_{T\in\mathcal{T}_h}\int_T \boldsymbol{f}\cdot\boldsymbol{v}_h dx.
\end{aligned} \tag{3.9}$$

We recall that

$$\begin{aligned}
&- 2\nu\sum_{e\in\mathcal{E}_h}\int_e \{D\boldsymbol{u}\}\boldsymbol{n}_e : [\boldsymbol{v}_h]d\sigma + \sum_{e\in\mathcal{E}_h}\int_e \{p\}\boldsymbol{n}_e\cdot[\boldsymbol{v}_h]d\sigma\\
&= -2\nu\sum_{e\in\mathcal{E}_h^0}\int_e \{D\boldsymbol{u}\}\boldsymbol{n}_e : [\boldsymbol{v}_h]d\sigma + \sum_{e\in\mathcal{E}_h^0}\int_e \{p\}\boldsymbol{n}_e\cdot[\boldsymbol{v}_h]d\sigma\\
&\quad - \sum_{e\in\mathcal{E}_h^\gamma}\int_e (\boldsymbol{T}(\boldsymbol{u}, p)\boldsymbol{n}_e)_{\boldsymbol{\tau}}\cdot\boldsymbol{v}_{\boldsymbol{\tau},h} d\sigma
\end{aligned}$$

which with (1.6) gives

$$
\begin{aligned}
&-2\nu\sum_{e\in\mathcal{E}_h}\int_e\{D\boldsymbol{u}\}\boldsymbol{n}_e:[\boldsymbol{v}_h]d\sigma+\sum_{e\in\mathcal{E}_h}\int_e\{p\}\boldsymbol{n}_e\cdot[\boldsymbol{v}_h]d\sigma\\
&=-2\nu\sum_{e\in\mathcal{E}_h^0}\int_e\{D\boldsymbol{u}\}\boldsymbol{n}_e:[\boldsymbol{v}_h]d\sigma+\sum_{e\in\mathcal{E}_h^0}\int_e\{p\}\boldsymbol{n}_e\cdot[\boldsymbol{v}_h]d\sigma\\
&+\sum_{e\in\mathcal{E}_h^\gamma}\int_e|K\boldsymbol{u}_{\boldsymbol{\tau}}|^{s-2}K\boldsymbol{u}_{\boldsymbol{\tau}}\cdot K\boldsymbol{v}_{\boldsymbol{\tau},h}d\sigma-\sum_{e\in\mathcal{E}_h^\gamma}\int_e g\boldsymbol{v}_{\boldsymbol{\tau},h}d\sigma.
\end{aligned}
$$

Returning to (3.9), we get the desired result. □

4 Solvability

In this section, we address the solvability of (3.6). But before that, we recall some well known results that will be important in the analysis. The following standard trace and inverse inequalities, which hold true on each element $T\in\mathcal{T}_h$, with diameter h_T, and for any face e of T (see [22]) will be important in analysis:

$$
\|\boldsymbol{v}\|_e\le c\left(h_T^{-1/2}\|\boldsymbol{v}\|_T+h_T^{1/2}\|\nabla\boldsymbol{v}\|_T\right)\quad\text{for all }\ \boldsymbol{v}\in H^1(T)\tag{4.1}
$$

$$
\|\boldsymbol{v}_h\|_{L^p(e)}\le ch_T^{-\frac{1}{p}+d\left(\frac{1}{p}-\frac{1}{r}\right)}\|\boldsymbol{v}_h\|_{L^r(T)}\ \text{ for all } r,\,p\in[1,\infty]\text{ and }\boldsymbol{v}\in\mathcal{P}_k(T).\tag{4.2}
$$

The bilinear form $A(\cdot,\cdot)$ and $B(\cdot,\cdot)$ satisfy several properties that are important for the analysis. Here, we briefly recall several well-known results. The proofs are omitted, for details see [23, 30, 40]. Now from Cauchy–Schwarz's inequality, Hölder's inequality, and (4.2), it hold that

$$
\begin{aligned}
&s(\boldsymbol{v}_h,\boldsymbol{w}_h)\le c\Big(\sum_{e\in\mathcal{E}_h^0}\frac{1}{h_e}\|[\boldsymbol{v}_h]\|_e^2\Big)^{1/2}\|D\boldsymbol{w}_h\|\ \text{ for all }(\boldsymbol{v}_h,\boldsymbol{w}_h)\in\mathbb{V}_h\times\mathbb{V}_h,\\
&\sum_{e\in\mathcal{E}_h^0}\int_e\{q_h\}[\boldsymbol{v}_h]\cdot\boldsymbol{n}_e ds\le c\Big(\sum_{e\in\mathcal{E}_h^0}\frac{1}{h_e}\|[\boldsymbol{v}_h]\|_e^2\Big)^{1/2}\|q_h\|\ \text{ for all }(\boldsymbol{v}_h,q_h)\in\mathbb{V}_h\times M_h\,.
\end{aligned}\tag{4.3}
$$

Now, using (4.3), we then deduce that

Lemma 4.1 (continuity of $A(\cdot,\cdot)$ and $B(\cdot,\cdot)$) *The bilinear forms $A(\cdot,\cdot)$ and $B(\cdot,\cdot)$ are continuous on $\mathbb{V}_h\times\mathbb{V}_h$ and $\mathbb{V}_h\times M_h$ respectively. More precisely, there exists c_I independent of the mesh size h such that*

$$
\begin{aligned}
A(\boldsymbol{v}_h,\boldsymbol{w}_h)&\le c_I|||\boldsymbol{v}_h|||_h|||\boldsymbol{w}_h|||_h\quad\text{for all }\ \boldsymbol{v}_h,\boldsymbol{w}_h\in\mathbb{V}_h,\\
B(\boldsymbol{v}_h,q_h)&\le c_I|||\boldsymbol{v}_h|||_h\|q_h\|\quad\text{for all }\ (\boldsymbol{v}_h,q_h)\in\mathbb{V}_h\times M_h.
\end{aligned}
$$

The coercivity of $A(\cdot,\cdot)$ is direct for *NIPG* and *IIPG* methods. We state that

Lemma 4.2 (coercivity of $A(\cdot,\cdot)$) *If $\epsilon_0 = 1$, then the non-symmetry of the form $A(\cdot,\cdot)$ yields the immediate coercivity property*

$$\begin{aligned} A^{NIPG}(\boldsymbol{v}_h, \boldsymbol{v}_h) =& 2\nu \sum_{T\in\mathcal{T}_h} \|D\boldsymbol{v}_h\|_T^2 + \sum_{e\in\mathcal{E}_h^0} \frac{\alpha}{h_e}\|[\boldsymbol{v}_h]\|_e^2 \\ &\geq \min(1, 2\nu)|||\boldsymbol{v}_h|||_h^2 \qquad \text{for } \alpha = 1. \end{aligned}$$

If $\epsilon_0 = -1$, then the bilinear form $A(\cdot,\cdot)$ is symmetric. In fact, we have

$$A^{SIPG}(\boldsymbol{v}_h, \boldsymbol{w}_h) = A^{NIPG}(\boldsymbol{v}_h, \boldsymbol{w}_h) - 2\nu \sum_{e\in\mathcal{E}_h^0} \int_e \{D\boldsymbol{w}_h\}\boldsymbol{n}_e \cdot [\boldsymbol{v}_h] d\sigma.$$

So the coercivity is proved if the penalty parameter α is chosen large enough. We give below an estimate for the admissible value of the penalty parameter α based on the following bound. There exists a constant $\gamma > 0$, that only depends on a trace and the constant in (4.2), such that

$$\sum_{e\in\mathcal{E}_h^0} \int_e \{D\boldsymbol{v}_h\}\boldsymbol{n}_e \cdot [\boldsymbol{v}_h] d\sigma \leq \gamma \Big(\sum_{e\in\mathcal{E}_h^0} \frac{1}{h_e}\|[\boldsymbol{v}_h]\|_e^2 \Big)^{1/2} \Big(\sum_{T\in\mathcal{T}_h} \|D\boldsymbol{v}_h\|_T^2 \Big)^{1/2}$$

Lemma 4.3 (coercivity of $A^{SIPG}(\cdot,\cdot)$) *If $\epsilon_0 = -1$. Assume that α is large enough such that*

$$\alpha \geq \gamma^2.$$

Then, we have

$$A^{SIPG}(\boldsymbol{v}_h, \boldsymbol{v}_h) \geq c(\gamma, \nu)|||\boldsymbol{v}_h|||_h^2 \qquad \text{for all } \boldsymbol{v}_h \in \mathbb{V}_h.$$

if $\epsilon_0 = 0$ then one can show that $A^{IIPG}(\cdot,\cdot)$ is coercive in $\mathbb{V}_h$ following Lemma 4.3.

Remark 4.1 From Lemmas 4.3 and 4.2, we can also show that the bilinear $A(\cdot,\cdot)$ is coercive on $\widetilde{\mathbb{V}}_h$.

From [23], for each number $p \in [2, \infty)$, there exists a constant $c(p)$ such that

$$\text{for all } \boldsymbol{v}_h \in \mathbb{V}_h\,,\ \|\boldsymbol{v}_h\|_{L^p(\Omega)} \leq c(p)|||\boldsymbol{v}_h|||_h. \tag{4.4}$$

With Cauchy–Schwarz's inequality, Hölder's inequality and (4.4), we deduce that

Lemma 4.4 *There exists a positive constant c independent of h such that for all $\boldsymbol{v}_h \in \mathbb{V}_h$*

$$F(\boldsymbol{v}_h) \leq \left(\sum_{T \in \mathcal{T}_h} \|\boldsymbol{f}\|_T^2 \right)^{1/2} |||\boldsymbol{v}_h|||_h + c\,|\Gamma|^{1/2}\,\|g\|_{L^\infty(\Gamma)} |||\boldsymbol{v}_h|||_h.$$

We now state and prove an inf-sup condition on $B(\cdot,\cdot)$.

Lemma 4.5 *Let the triangulation $\mathcal{T}_h$ satisfies (3.1). There exists $\beta^* > 0$, independent of h such that*

$$\forall q_h \in M_h, \quad \beta^* \|q_h\| \leq \sup_{\boldsymbol{v}_h \in \widetilde{\mathbb{V}}_h} \frac{B(\boldsymbol{v}_h, q_h)}{|||\boldsymbol{v}_h|||_h}. \tag{4.5}$$

Proof The proof is not new, and we reproduce it for the readers sake. It is worth observing that this is equivalent to showing that, for any given $q_h \in M_h$, there exists $\boldsymbol{w}_h \in \widetilde{\mathbb{V}}_h$ and positive constants c_1, c_2 such that

$$B(\boldsymbol{w}_h, q_h) \geq c_1 \|q_h\|^2 \quad , \quad |||\boldsymbol{w}_h|||_h \leq c_2 \|q_h\|. \tag{4.6}$$

Fix $q_h \in M_h$, hence there is $\widetilde{\boldsymbol{v}} \in H_0^1(\Omega)^2$ and a constant c (independent of h) such that

$$\operatorname{div} \widetilde{\boldsymbol{v}} = q_h \quad , \quad \|\nabla \widetilde{\boldsymbol{v}}\| \leq c \|q_h\|. \tag{4.7}$$

Take $\boldsymbol{w}_h = \Pi \widetilde{\boldsymbol{v}}$ with Π the operator of Raviart-Thomas satisfying (3.4). From the definition of $B(\cdot,\cdot)$, the first two relations in (3.4) and the first relation in (4.7), we have

$$B(\boldsymbol{w}_h, q_h) = b(\boldsymbol{w}_h, q_h) + \sum_{e \in \mathcal{E}_h^0} \int_e \{q_h\}[\boldsymbol{w}_h] \cdot \boldsymbol{n}_e d\sigma = \|q_h\|^2. \tag{4.8}$$

Next, we bound $|||\boldsymbol{w}_h|||_h^2 = \sum_{K \in \mathcal{T}_h} \|D\boldsymbol{w}_h\|_K^2 + \sum_{e \in \mathcal{E}_h^0} \frac{1}{h_e} \|[\boldsymbol{w}_h]\|_e^2$. From the fourth relation in (3.4) and (4.7), we have

$$\begin{aligned} \sum_{T \in \mathcal{T}_h} \|D\boldsymbol{w}_h\|_T^2 &\leq \sum_{T \in \mathcal{T}_h} \|\nabla \boldsymbol{w}_h\|_T^2 \leq 2 \sum_{T \in \mathcal{T}_h} \|\nabla(\Pi\widetilde{\boldsymbol{v}} - \widetilde{\boldsymbol{v}})\|_T^2 + 2 \sum_{T \in \mathcal{T}_h} \|\nabla \widetilde{\boldsymbol{v}}\|_T^2 \\ &\leq c \sum_{T \in \mathcal{T}_h} \|\nabla \widetilde{\boldsymbol{v}}\|_T^2 \\ &\leq c \|q_h\|^2. \end{aligned}$$

Finally, the jump term is bounded using the fourth relation in (3.4) and (4.7) as follows

$$\sum_{e\in\mathcal{E}_h^0}\frac{1}{h_e}\|[\boldsymbol{w}_h]\|_e^2=\sum_{e\in\mathcal{E}_h^0}\frac{1}{h_e}\|[\Pi\widetilde{\boldsymbol{v}}]\|_e^2=\sum_{e\in\mathcal{E}_h^0}\frac{1}{h_e}\|[\Pi\widetilde{\boldsymbol{v}}-\widetilde{\boldsymbol{v}}]\|_e^2\leq c\|\nabla\widetilde{\boldsymbol{v}}\|^2\leq c\|q_h\|^2.$$

We then conclude that

$$|||\boldsymbol{w}_h|||_h\leq c\|q_h\|. \tag{4.9}$$

So, (4.8) and (4.9) gives (4.6). This ends the proof. □

The variational problem (3.6) is a nonlinear, hence it can be solved by Brouwer's fixed point theorem. To this end, we claim that

Theorem 4.1 *The variational problem* (3.6) *has a unique solution* $(\boldsymbol{u}_h,\,p_h)\in\mathbb{V}_h\times M_h$, *which furthermore satisfy*

$$c|||\boldsymbol{u}_h|||_h^2+\sum_{e\in\mathcal{E}_h^\gamma}\int_e\left|K\boldsymbol{u}_{\boldsymbol{\tau},h}\right|^s d\sigma\leq\sum_{T\in\mathcal{T}_h}\|\boldsymbol{f}\|_T^2+|\Gamma|\|g\|_{L^\infty(\Gamma)}^2,$$

and

$$\|p_h\|\leq c|||\boldsymbol{u}_h|||_h+c\|K\|_{L^\infty(\Gamma)}^s|||\boldsymbol{u}_h|||_h^{s-1}+c\|g\|_{L^\infty(\Gamma)}|\Gamma|^{1/2}+c\left(\sum_{T\in\mathcal{T}_h}\|\boldsymbol{f}\|_T^2\right)^{1/2}.$$

Proof We will use Brouwer's fixed point to obtain the solvability of (3.6). The discrete kernel of the bilinear form $B(\cdot,\cdot)$ is the set

$$\mathcal{Z}_h=\Big\{\boldsymbol{v}_h\in\mathbb{V}_h:\quad\text{for all } q_h\in M_h,\;\; B(\boldsymbol{v}_h,q_h)=0\Big\}.$$

So, for fixed $\boldsymbol{w}_h\in\mathcal{Z}_h$, we define $\mathcal{H}(\boldsymbol{w}_h)\in\mathcal{Z}_h$ by:

$$\begin{cases}\text{for all } \boldsymbol{v}_h\in\mathcal{Z}_h\,,\\ \mathcal{H}(\boldsymbol{w}_h)\boldsymbol{v}_h=A(\boldsymbol{w}_h,\boldsymbol{v}_h)+H(\boldsymbol{w}_h)\boldsymbol{v}_h-F(\boldsymbol{v}_h).\end{cases}$$

• $\mathcal{H}$ defines a continuous mapping from $\mathcal{Z}_h\longrightarrow\mathcal{Z}_h$.
Indeed, Let $\boldsymbol{w}_h^1$, $\boldsymbol{w}_h^2$ and $\boldsymbol{v}_h$ elements of $\mathbb{V}_h$. We have from Lemma 4.1

$$\begin{aligned}(\mathcal{H}(\boldsymbol{w}_h^1)-\mathcal{H}(\boldsymbol{w}_h^2)\boldsymbol{v}_h&=A(\boldsymbol{w}_h^1-\boldsymbol{w}_h^2,\boldsymbol{v}_h)+\Big(H(\boldsymbol{w}_h^1)-H(\boldsymbol{w}_h^2)\Big)\boldsymbol{v}_h\\&\leq c|||\boldsymbol{w}_h^1-\boldsymbol{w}_h^2|||_h|||\boldsymbol{v}_h|||_h+\Big(H(\boldsymbol{w}_h^1)-H(\boldsymbol{w}_h^2)\Big)\boldsymbol{v}_h\end{aligned}$$

We need to bound $\left(H(\boldsymbol{w}_h^1) - H(\boldsymbol{w}_h^2)\right)\boldsymbol{v}_h$. For that purpose, using Cauchy–Schwarz's inequality, Hölder's inequality, (4.2), (2.4), the trace's theorem, and (4.4), one gets

$$\begin{aligned}
\left(H(\boldsymbol{w}_h^1) - H(\boldsymbol{w}_h^2)\right)\boldsymbol{v}_h &= \sum_{e\in\mathcal{E}_h^\gamma}\int_e \left(\left|K\boldsymbol{w}_{\boldsymbol{\tau}h}^1\right|^{s-2}K\boldsymbol{w}_{\boldsymbol{\tau}h}^1 - \left|K\boldsymbol{w}_{\boldsymbol{\tau}h}^2\right|^{s-2}K\boldsymbol{w}_{\boldsymbol{\tau}h}^2\right)\cdot K\boldsymbol{v}_{\boldsymbol{\tau}h}d\sigma\\
&\le c\|K\|_{L^\infty(\Gamma)}^s \sum_{e\in\mathcal{E}_h^\gamma}\int_e \left|\boldsymbol{w}_{\boldsymbol{\tau}h}^1 - \boldsymbol{w}_{\boldsymbol{\tau}h}^2\right|^{s-1}|\boldsymbol{v}_{\boldsymbol{\tau}h}|d\sigma\\
&\le c\|K\|_{L^\infty(\Gamma)}^s \left(\sum_{e\in\mathcal{E}_h^\gamma}\left\|\boldsymbol{w}_{\boldsymbol{\tau}h}^1 - \boldsymbol{w}_{\boldsymbol{\tau}h}^2\right\|_e^{2(s-1)}\right)^{1/2}\left(\sum_{e\in\mathcal{E}_h^\gamma}\|\boldsymbol{v}_{\boldsymbol{\tau}h}\|_e^2\right)^{1/2}\\
&\le c\|K\|_{L^\infty(\Gamma)}^s \left\|\boldsymbol{w}_{\boldsymbol{\tau}h}^1 - \boldsymbol{w}_{\boldsymbol{\tau}h}^2\right\|_\Gamma^{(s-1)}\|\boldsymbol{v}_{\boldsymbol{\tau}h}\|_\Gamma\\
&\le c\|\boldsymbol{w}_{\boldsymbol{\tau}h}^1 - \boldsymbol{w}_{\boldsymbol{\tau}h}^2\|_\Gamma^{s-1}|||\boldsymbol{v}_h|||_h,
\end{aligned}$$

which implies that

$$(\mathcal{H}(\boldsymbol{w}^1) - \mathcal{H}(\boldsymbol{w}^2)\boldsymbol{v} \le c|||\boldsymbol{w}_h^1 - \boldsymbol{w}_h^2|||_h|||\boldsymbol{v}_h|||_h + c\|\boldsymbol{w}_{\boldsymbol{\tau}h}^1 - \boldsymbol{w}_{\boldsymbol{\tau}h}^2\|_\Gamma^{s-1}|||\boldsymbol{v}_h|||_h.$$

• $\mathcal{H}(\boldsymbol{v}_h)\boldsymbol{v}_h$ is bounded from below. Indeed for $\boldsymbol{v}_h \in \mathbb{V}_h$,

$$\begin{aligned}
\mathcal{H}(\boldsymbol{v}_h)\boldsymbol{v}_h =& A(\boldsymbol{v}_h,\boldsymbol{v}_h) + H(\boldsymbol{v}_h)\boldsymbol{v}_h - F(\boldsymbol{v}_h)\\
\ge& c|||\boldsymbol{v}_h|||_h^2 + \sum_{e\in\mathcal{E}_h^\gamma}\int_e \left|K\boldsymbol{v}_{\boldsymbol{\tau},h}\right|^s d\sigma - c\left(\sum_{T\in\mathcal{T}_h}\|\boldsymbol{f}\|_T^2\right)^{1/2}|||\boldsymbol{v}_h|||_h - c\,|\Gamma|^{1/2}\|g\|_{L^\infty(\Gamma)}|||\boldsymbol{v}_h|||_h\\
\ge& |||\boldsymbol{v}_h|||_h\left(c|||\boldsymbol{v}_h|||_h - c\left(\sum_{T\in\mathcal{T}_h}\|\boldsymbol{f}\|_T^2\right)^{1/2} - c\|g\|_{L^\infty(\Gamma)}|\Gamma|^{1/2}\right).
\end{aligned}$$

Thus for $|||\boldsymbol{v}_h|||_h = r$ with $r > c\left(\sum_{T\in\mathcal{T}_h}\|\boldsymbol{f}\|_T^2\right)^{1/2} + c\|g\|_{L^\infty(\Gamma)}|\Gamma|^{1/2}$, $\mathcal{H}(\boldsymbol{v}_h)\boldsymbol{v}_h$ is non negative. By Brouwer's Fixed Point Theorem, this proves the existence of at least one solution $\boldsymbol{u}_h \in \mathcal{Z}_h$ of $\mathcal{H}(\boldsymbol{u}_h)\boldsymbol{v}_h = 0$ for all $\boldsymbol{v}_h \in \mathcal{Z}_h$. The pressure is constructed in the usual way thank to the inf-sup condition (4.5). The estimates are obtained by taking $\boldsymbol{v}_h = \boldsymbol{u}_h$ in (3.6), and use the inf-sup condition (4.5).
As for uniqueness, we assume that (3.6) has two solutions, say, $(\boldsymbol{u}^1, p^1)$ and $(\boldsymbol{u}^2, p^2)$. Then

$$\begin{cases}
\text{for all } (\boldsymbol{v}_h, q_h) \in \mathbb{V}_h \times M_h,\\
A(\boldsymbol{u}^1 - \boldsymbol{u}^2, \boldsymbol{v}_h) + B(\boldsymbol{v}_h, p^1 - p^2) + \left(H(\boldsymbol{u}^1) - H(\boldsymbol{u}^2)\right)\boldsymbol{v}_h = 0,\\
B(\boldsymbol{u}^1 - \boldsymbol{u}^2, q_h) = 0.
\end{cases} \tag{4.10}$$

We take successively $\boldsymbol{v}_h = \boldsymbol{u}^1$ and $\boldsymbol{u}^2$ in (4.10), subtracting the resulting equations (having in mind the second equation in (4.10) for $q_h = p^1 - p^2$), we obtain

$$A(\boldsymbol{u}^1 - \boldsymbol{u}^2, \boldsymbol{u}^1 - \boldsymbol{u}^2) + \underbrace{\left(H(\boldsymbol{u}^1) - H(\boldsymbol{u}^2)\right)(\boldsymbol{u}^1 - \boldsymbol{u}^2)}_{\geq 0} = 0,$$

which implies that $|||\boldsymbol{u}^1 - \boldsymbol{u}^2|||_h^2 = 0$, so $\boldsymbol{u}^1 = \boldsymbol{u}^2$. Returning to (4.10), one obtains that

$$\begin{cases} \text{for all } \boldsymbol{v}_h \in \mathbb{V}_h, \\ B(\boldsymbol{v}_h, p^1 - p^2) = 0, \end{cases}$$

together with the inf-sup condition (4.5) leads to $p^1 = p^2$. □

Remark 4.2 For non linear problems, uniqueness is often conditional and extra regularity of the solution is sometime required. But in this situation, the nonlinear term is monotone, and nothing is required.

5 A priori error estimate

We assume that $(\boldsymbol{u}, p)$ is the unique solution constructed in Theorem 2.1, while $(\boldsymbol{u}_h, p_h)$ is the DG solution constructed in Theorem 4.1. In this section, our goal is to bound the errors $|||\boldsymbol{u} - \boldsymbol{u}_h|||_h$ and $\|p - p_h\|$. Before stating the main result of this research, we have the following result based on Lemma 4.5 (similar ideas are used in [23, 43]):

Lemma 5.1 *There exists an approximation operator $R_h \in \mathcal{L}(H^1(\Omega)^2; \widetilde{\mathbb{V}}_h)$ satisfying*

$$\begin{aligned} &\forall (\boldsymbol{v}, q_h) \in H^1(\Omega)^2 \times M_h, \quad B(R_h\boldsymbol{v} - \boldsymbol{v}, q_h) = 0, \\ &\forall (s, \boldsymbol{v}) \in [1, k+1] \times H^s(\Omega)^2\,, \ |||R_h\boldsymbol{v} - \boldsymbol{v}|||_h \leq ch^{s-1}|\boldsymbol{v}|_{H^s(\Omega)}, \\ &\forall \boldsymbol{v} \in H^1(\Omega)^2, \ |||R_h\boldsymbol{v}|||_h \leq c\|D\boldsymbol{v}\|. \end{aligned}$$

Proof Let $\pi_h \in \mathcal{L}(H^1(\Omega)^2; \mathbb{V} \cap \widetilde{\mathbb{V}}_h)$ be the Scott–Zhang's interpolation operator (see [44]), and set

$$R_h\boldsymbol{v} = \pi_h\boldsymbol{v} + \boldsymbol{x}_h(\boldsymbol{v}) \ \text{ for all } \boldsymbol{v} \in \mathbb{V}$$

with $\boldsymbol{x}_h(\boldsymbol{v}) \in \widetilde{\mathbb{V}}_h$ taken (hopefully) such that

$$\text{for all } (\boldsymbol{v}, q_h) \in \mathbb{V} \times M_h, \quad B(\pi_h\boldsymbol{v} + \boldsymbol{x}_h(\boldsymbol{v}) - \boldsymbol{v}, q_h) = 0\,. \tag{5.1}$$

Ones observes that (5.1) is equivalent to;

$$\begin{cases} \text{for all } (\boldsymbol{v}, q_h) \in H^1(\Omega)^2 \times M_h, \\ B(\boldsymbol{x}_h(\boldsymbol{v}), q_h) = B(\boldsymbol{v} - \pi_h \boldsymbol{v}, q_h) = \displaystyle\int_\Omega \operatorname{div}(\boldsymbol{v} - \pi_h \boldsymbol{v}) q_h dx + \sum_{e \in \mathcal{E}_h^0} \int_e \{q_h\} \underbrace{[\boldsymbol{v} - \pi_h \boldsymbol{v}]}_{=0} \cdot \boldsymbol{n}_e d\sigma. \end{cases} \tag{5.2}$$

From Babuska–Brezzi's approach for mixed problems (see [5, 22]), (5.2) has at least solution $\boldsymbol{x}_h(\boldsymbol{v}) \in \widetilde{\mathbb{V}}_h$, which is unique in $(\mathcal{Z}_h)^\perp$ (the orthogonal being taken with respect to $|||\cdot|||_h$). From Lemma 4.5, there exists β^* independent of h such that

$$|||\boldsymbol{x}_h(\boldsymbol{v})|||_h \leq \frac{1}{\beta^*} \| \operatorname{div}(\boldsymbol{v} - \pi_h \boldsymbol{v})\|. \tag{5.3}$$

Then, the first assertion in Lemma 5.1 follows from (5.2).
The second assertion is a consequence of the approximation properties of π_h.
Using the triangle's inequality, approximation properties of π_h, (5.3) one gets

$$|||R_h \boldsymbol{v}|||_h \leq |||\pi_h \boldsymbol{v}|||_h + |||x_h(\boldsymbol{v})|||_h \leq |||\pi_h \boldsymbol{v}|||_h + \frac{1}{\beta^*} \| \operatorname{div}(\boldsymbol{v} - \pi_h \boldsymbol{v})\| \leq c \|\nabla \boldsymbol{v}\|$$

this ends the proof. □

Remark 5.1 For $k = 1, 2, 3$, Girault–Riviere–Wheeler in [23] have constructed another operator R_h that is based on the nonconforming elements of [12, 13, 19]. This operator is quasi-local and hence satisfies optimal approximation properties in L^r and $W^{1,r}$ for any number $r \geq 2$, without restricting the mesh or the domain. However, this is not fundamental here, and therefore, we do not use it in the present work.

The following result establishes a uniform error estimate with respect to s between the exact solution and the DG-solution.

Theorem 5.1 *Let $(\boldsymbol{u}, p)$ be the unique solution of (2.2) given by Theorem 2.1 and satisfying $(\boldsymbol{u}, p) \in H^2(\Omega)^2 \times H^1(\Omega)$. Then the DG solution $(\boldsymbol{u}_h, p_h)$ constructed in Theorem 4.1 satisfy*

$$\begin{aligned} |||\boldsymbol{u} - \boldsymbol{u}_h|||_h + \|\boldsymbol{u}_\tau - \boldsymbol{u}_{\tau,h}\|_\Gamma \leq c \Big(\sum_{T \in \mathcal{T}_h} \|p - r_h p\|_T^2 + h_T^2 \|\nabla(p - r_h p)\|_T^2 \Big)^{1/2} + c|||\boldsymbol{u} - R_h \boldsymbol{u}|||_h \\ + c \left(\sum_{e \in \mathcal{E}_h^\gamma} \|\boldsymbol{u}_\tau - (R_h \boldsymbol{u})_\tau\|_e \right)^{1/2}, \end{aligned}$$

and

$$\begin{aligned} \|p - p_h\| \leq c \Big(\sum_{T \in \mathcal{T}_h} \|p - r_h p\|_T^2 + h_T^2 \|\nabla(p - r_h p)\|_T^2 \Big)^{1/2} + c|||\boldsymbol{u} - R_h \boldsymbol{u}|||_h \\ + c \left(\sum_{e \in \mathcal{E}_h^\gamma} \|\boldsymbol{u}_\tau - (R_h \boldsymbol{u})_\tau\|_e \right)^{1/2}. \end{aligned}$$

Proof Let us denote the numerical and approximation errors by $\boldsymbol{e}_u = \boldsymbol{u} - \boldsymbol{u}_h$ and $e_p = p - p_h$. We adopt the following decomposition of the errors

$$\boldsymbol{e}_u = \boldsymbol{u} - R_h\boldsymbol{u} + R_h\boldsymbol{u} - \boldsymbol{u}_h \text{ and } e_p = p - r_h p + r_h p - p_h.$$

We note that the terms $\boldsymbol{u} - R_h\boldsymbol{u}$ and $p - r_h p$ are bounded by a priori error estimate in (3.4) and (3.3), respectively. Thus, we need to find the bounds for $R_h\boldsymbol{u} - \boldsymbol{u}_h$ and $r_h p - p_h$.

Step 1. Inf-sup condition on $B(\cdot,\cdot)$. We first bound $\|p_h - r_h p\|$. We recall that $p_h - r_h p$ is an element of M_h, and the couple $(M_h, \widetilde{\mathbb{V}}_h \cap \{\boldsymbol{v}_h|_{\partial\Omega} = \boldsymbol{0}\})$ is inf-sup stable. Then

$$\begin{aligned}\beta\|p_h - r_h p\| &\le \sup_{\boldsymbol{v}_h\in\widetilde{\mathbb{V}}_h\cap\{\boldsymbol{v}_h|_{\partial\Omega}=0\}} \frac{B(\boldsymbol{v}_h,\, p_h - r_h p)}{|||\boldsymbol{v}_h|||_h} \\ &\le \sup_{\boldsymbol{v}_h\in\widetilde{\mathbb{V}}_h\cap\{\boldsymbol{v}_h|_{\partial\Omega}=0\}} \frac{B(\boldsymbol{v}_h,\, p_h - p) + B(\boldsymbol{v}_h,\, p - r_h p)}{|||\boldsymbol{v}_h|||_h}.\end{aligned} \tag{5.4}$$

From the consistency equation (see Lemma 3.1), we deduce that

$$\begin{cases}\text{for all } (\boldsymbol{v}_h, q_h) \in \mathbb{V}_h \times M_h, \\ A(\boldsymbol{u}_h - \boldsymbol{u}, \boldsymbol{v}_h) + B(\boldsymbol{v}_h,\, p_h - p) + (H(\boldsymbol{u}) - H(\boldsymbol{u}_h))\boldsymbol{v}_h = 0 \\ B(\boldsymbol{u}_h - \boldsymbol{u}, q_h) = 0.\end{cases} \tag{5.5}$$

We then deduce that $B(\boldsymbol{v}_h,\, p_h - p) = A(\boldsymbol{u} - \boldsymbol{u}_h, \boldsymbol{v}_h)$ for all $\boldsymbol{v}_h \in \widetilde{\mathbb{V}}_h \cap \{\boldsymbol{v}_h|_{\partial\Omega} = 0\}$. Returning to (5.4) with (5.5) and using Lemmas 4.5 and 4.1, one obtains

$$\beta\|p_h - r_h p\| \le \sup_{\boldsymbol{v}_h\in\widetilde{\mathbb{V}}_h\cap\{\boldsymbol{v}_h|_{\partial\Omega}=0\}} \frac{A(\boldsymbol{u} - \boldsymbol{u}_h, \boldsymbol{v}_h) + B(\boldsymbol{v}_h,\, p - r_h p)}{|||\boldsymbol{v}_h|||_h}. \tag{5.6}$$

We now bound the right hand side of (5.6). From Cauchy–Schwarz's inequality, Hölder's inequality, we easily get

$$A(\boldsymbol{u} - \boldsymbol{u}_h, \boldsymbol{v}_h) \le c|||\boldsymbol{u} - \boldsymbol{u}_h|||_h|||\boldsymbol{v}_h|||_h.$$

The second term on the right hand side of (5.6) cannot be treated using Lemma 4.1, because $p - r_h p$ is not an element of M_h. Instead, with Cauchy–Schwarz's inequality, Hölder's inequality, and (4.1), we have

$$\begin{aligned}B(\boldsymbol{v}_h,\, p - r_h p) &= -\sum_{T\in\mathcal{T}_h}\int_T (p - r_h p)\,\mathrm{div}\,\boldsymbol{v}_h dx + \sum_{e\in\mathcal{E}_h^0}\int_e \{p - r_h p\}[\boldsymbol{v}_h]\cdot\boldsymbol{n}_e ds \\ &\le \Big(\sum_{T\in\mathcal{T}_h}\|p - r_h p\|_T^2\Big)^{1/2}\Big(\sum_{T\in\mathcal{T}_h}\|\nabla\boldsymbol{v}_h\|_T^2\Big)^{1/2}\end{aligned}$$

$$
\begin{aligned}
&+c\Big(\sum_{T\in\mathcal{T}_h}\|p-r_hp\|_T^2+h_T^2\|\nabla(p-r_hp)\|_T^2\Big)^{1/2}\\
&\quad\times\Big(\sum_{e\in\mathcal{E}_h^0}\frac{1}{h_e}\|[\boldsymbol{v}_h]\|_e^2\Big)^{1/2}\\
&\leq\ c\Big(\sum_{T\in\mathcal{T}_h}\|p-r_hp\|_T^2+h_T^2\|\nabla(p-r_hp)\|_T^2\Big)^{1/2}|||\boldsymbol{v}_h|||_h. \qquad (5.7)
\end{aligned}
$$

So, returning to (5.6), one obtains after using the triangle's inequality

$$
\begin{aligned}
\beta\|p_h-r_hp\|\leq c|||\boldsymbol{u}-R_h\boldsymbol{u}|||_h+c|||R_h\boldsymbol{u}-\boldsymbol{u}_h|||_h\\
+c\Big(\sum_{T\in\mathcal{T}_h}\|p-r_hp\|_T^2+h_T^2\|\nabla(p-r_hp)\|_T^2\Big)^{1/2}. \qquad (5.8)
\end{aligned}
$$

Step 2. coercivity of $A(\cdot,\cdot)$. We recall that $R_h\boldsymbol{u}-\boldsymbol{u}_h\in\widetilde{\mathbb{V}}_h$, hence Remark 4.1 is applicable, and

$$
\begin{aligned}
c|||\boldsymbol{u}_h-R_h\boldsymbol{u}|||_h^2&\leq A(\boldsymbol{u}_h-R_h\boldsymbol{u},\boldsymbol{u}_h-R_h\boldsymbol{u})\\
&=A(\boldsymbol{u}_h-\boldsymbol{u},\boldsymbol{u}_h-R_h\boldsymbol{u})+A(\boldsymbol{u}-R_h\boldsymbol{u},\boldsymbol{u}_h-R_h\boldsymbol{u}) \qquad (5.9)\\
&=T_1+T_2.
\end{aligned}
$$

We now bound T_1 and T_2. Starting with T_2 and using the same arguments presented in Lemma 4.1, we have

$$
T_2=A(\boldsymbol{u}-R_h\boldsymbol{u},\boldsymbol{u}_h-R_h\boldsymbol{u})\leq c|||\boldsymbol{u}-R_h\boldsymbol{u}|||_h|||\boldsymbol{u}_h-R_h\boldsymbol{u}|||_h. \qquad (5.10)
$$

From Lemma 3.1 (consistency equation), one deduces that (taking $\boldsymbol{v}_h=\boldsymbol{u}_h-R_h\boldsymbol{u}$)

$$
A(\boldsymbol{u},\boldsymbol{u}_h-R_h\boldsymbol{u})=F(\boldsymbol{u}_h-R_h\boldsymbol{u})-B(\boldsymbol{u}_h-R_h\boldsymbol{u},p)-H(\boldsymbol{u})(\boldsymbol{u}_h-R_h\boldsymbol{u}). \qquad (5.11)
$$

But we recall that $\boldsymbol{u}_h$ satisfies

$$
A(\boldsymbol{u}_h,\boldsymbol{u}_h-R_h\boldsymbol{u})=F(\boldsymbol{u}_h-R_h\boldsymbol{u})-B(\boldsymbol{u}_h-R_h\boldsymbol{u},p_h)-H(\boldsymbol{u}_h)(\boldsymbol{u}_h-R_h\boldsymbol{u}). \qquad (5.12)
$$

Thus (5.11) and (5.12) implies that

$$
\begin{aligned}
T_1&=A(\boldsymbol{u}_h-\boldsymbol{u},\boldsymbol{u}_h-R_h\boldsymbol{u})\\
&=A(\boldsymbol{u}_h,\boldsymbol{u}_h-R_h\boldsymbol{u})-A(\boldsymbol{u},\boldsymbol{u}_h-R_h\boldsymbol{u}) \qquad (5.13)\\
&=B(\boldsymbol{u}_h-R_h\boldsymbol{u},p-p_h)+(H(\boldsymbol{u})-H(\boldsymbol{u}_h))(\boldsymbol{u}_h-R_h\boldsymbol{u}).
\end{aligned}
$$

Using the second equation in (5.5) and the first relation in Lemma 5.1, we deduce that

$$B(\boldsymbol{u}_h - R_h\boldsymbol{u},\, p - p_h) = B(\boldsymbol{u}_h - R_h\boldsymbol{u},\, p - r_h p). \tag{5.14}$$

Thus (5.14) together with (5.13) gives

$$T_1 = B(\boldsymbol{u}_h - R_h\boldsymbol{u},\, p - r_h p) + (H(\boldsymbol{u}) - H(\boldsymbol{u}_h))\,(\boldsymbol{u}_h - R_h\boldsymbol{u}). \tag{5.15}$$

We re-write (5.15) as follows

$$\begin{aligned} &T_1 + (H(\boldsymbol{u}) - H(\boldsymbol{u}_h))\,(\boldsymbol{u} - \boldsymbol{u}_h) \\ &\quad = B(\boldsymbol{u}_h - R_h\boldsymbol{u},\, p - r_h p) + (H(\boldsymbol{u}) - H(\boldsymbol{u}_h))\,(\boldsymbol{u} - R_h\boldsymbol{u}). \end{aligned} \tag{5.16}$$

From (2.3), and it can be shown that (see [41]): there exist α_1, α_2 two positive constants such that

$$\alpha_1 \frac{\|\boldsymbol{u}_{\boldsymbol{\tau}} - \boldsymbol{u}_{\boldsymbol{\tau},h}\|_\Gamma^2}{\alpha_2 + \|\boldsymbol{u}_{\boldsymbol{\tau}}\|_\Gamma^{2-s} + \|\boldsymbol{u}_{\boldsymbol{\tau},h}\|_\Gamma^{2-s}} \le (H(\boldsymbol{u}) - H(\boldsymbol{u}_h))\,(\boldsymbol{u} - \boldsymbol{u}_h).$$

Thus returning to (5.16) and using the inequality (5.7), we obtain

$$\begin{aligned} &T_1 + \alpha_1 \frac{\|\boldsymbol{u}_{\boldsymbol{\tau}} - \boldsymbol{u}_{\boldsymbol{\tau},h}\|_\Gamma^2}{\alpha_2 + \|\boldsymbol{u}_{\boldsymbol{\tau}}\|_\Gamma^{2-s} + \|\boldsymbol{u}_{\boldsymbol{\tau},h}\|_\Gamma^{2-s}} \\ &\quad \le c|||\boldsymbol{u}_h - R_h\boldsymbol{u}|||_h \Big(\sum_{T\in\mathcal{T}_h} \|p - r_h p\|_T^2 + h_T^2 \|\nabla(p - r_h p)\|_T^2 \Big)^{1/2} \\ &\quad + (H(\boldsymbol{u}) - H(\boldsymbol{u}_h))\,(\boldsymbol{u} - R_h\boldsymbol{u}). \end{aligned} \tag{5.17}$$

The second term in the right hand side of (5.17) is bounded as follows

$$\begin{aligned} (H(\boldsymbol{u}) - H(\boldsymbol{u}_h))\,(\boldsymbol{u} - R_h\boldsymbol{u}) &= \sum_{e\in\mathcal{E}_h^\gamma} \int_e \Big(|K\boldsymbol{u}_{\boldsymbol{\tau}}|^{s-2} K\boldsymbol{u}_{\boldsymbol{\tau}} - \big|K\boldsymbol{u}_{\boldsymbol{\tau},h}\big|^{s-2} K\boldsymbol{u}_{\boldsymbol{\tau},h} \Big) \cdot K(\boldsymbol{u}_{\boldsymbol{\tau}} - (R_h\boldsymbol{u})_{\boldsymbol{\tau}}) d\sigma \\ &\le \sum_{e\in\mathcal{E}_h^\gamma} \int_e \Big| |K\boldsymbol{u}_{\boldsymbol{\tau}}|^{s-2} K\boldsymbol{u}_{\boldsymbol{\tau}} - \big|K\boldsymbol{u}_{\boldsymbol{\tau},h}\big|^{s-2} K\boldsymbol{u}_{\boldsymbol{\tau},h} \Big|\, |K(\boldsymbol{u}_{\boldsymbol{\tau}} - (R_h\boldsymbol{u})_{\boldsymbol{\tau}})| d\sigma \\ &\le c\|K\|_{L^\infty(\Gamma)}^s \sum_{e\in\mathcal{E}_h^\gamma} \int_e \big|\boldsymbol{u}_{\boldsymbol{\tau}} - \boldsymbol{u}_{\boldsymbol{\tau},h}\big|^{s-1}\, |\boldsymbol{u}_{\boldsymbol{\tau}} - (R_h\boldsymbol{u})_{\boldsymbol{\tau}}| d\sigma \\ &\le c\|K\|_{L^\infty(\Gamma)} \sum_{e\in\mathcal{E}_h^\gamma} \Big(\int_e \big|\boldsymbol{u}_{\boldsymbol{\tau}} - \boldsymbol{u}_{\boldsymbol{\tau},h}\big|^{2(s-1)} \Big)^{1/2} \Big(\int_e |\boldsymbol{u}_{\boldsymbol{\tau}} - (R_h\boldsymbol{u})_{\boldsymbol{\tau}}|^2 \Big)^{1/2} \\ &\le c\|K\|_{L^\infty(\Gamma)}^s \sum_{e\in\mathcal{E}_h^\gamma} \big\|\boldsymbol{u}_{\boldsymbol{\tau}} - \boldsymbol{u}_{\boldsymbol{\tau},h}\big\|_e^{s-1}\, \|\boldsymbol{u}_{\boldsymbol{\tau}} - (R_h\boldsymbol{u})_{\boldsymbol{\tau}}\|_e . \end{aligned}$$

So, the inequality (5.17) gives

$$
\begin{aligned}
T_1+\alpha_1 \frac{\|\boldsymbol{u}_{\boldsymbol{\tau}}-\boldsymbol{u}_{\boldsymbol{\tau},h}\|_{\Gamma}^2}{\alpha_2+\|\boldsymbol{u}_{\boldsymbol{\tau}}\|_{\Gamma}^{2-s}+\|\boldsymbol{u}_{\boldsymbol{\tau},h}\|_{\Gamma}^{2-s}} & \\
\leq c|||\boldsymbol{u}_h-R_h\boldsymbol{u}|||_h\Big(\sum_{T\in\mathcal{T}_h}\|p-r_hp\|_T^2+h_T^2\|\nabla(p-r_hp)\|_T^2\Big)^{1/2} & \\
+c\left(\sum_{e\in\mathcal{E}_h^{\gamma}}\|\boldsymbol{u}_{\boldsymbol{\tau}}\|_e^{s-1}+\left\|\boldsymbol{u}_{\boldsymbol{\tau},h}\right\|_e^{s-1}\right)\left(\sum_{e\in\mathcal{E}_h^{\gamma}}\|\boldsymbol{u}_{\boldsymbol{\tau}}-(R_h\boldsymbol{u})_{\boldsymbol{\tau}}\|_e^2\right)^{1/2}. &
\end{aligned}
\tag{5.18}
$$

We replace (5.18) and (5.10) in (5.9), using the bounds on $\|\boldsymbol{u}_{\boldsymbol{\tau}}\|_e$ and $\left\|\boldsymbol{u}_{\boldsymbol{\tau},h}\right\|_e$, and Young's inequality, one obtains

$$
\begin{aligned}
|||\boldsymbol{u}_h-R_h\boldsymbol{u}|||_h \leq c\Big(\sum_{T\in\mathcal{T}_h}\|p-r_hp\|_T^2+h_T^2\|\nabla(p-r_hp)\|_T^2\Big)^{1/2}+c|||\boldsymbol{u}-R_h\boldsymbol{u}|||_h & \\
+c\left(\sum_{e\in\mathcal{E}_h^{\gamma}}\|\boldsymbol{u}_{\boldsymbol{\tau}}-(R_h\boldsymbol{u})_{\boldsymbol{\tau}}\|_e\right)^{1/2}, &
\end{aligned}
\tag{5.19}
$$

which together with triangle's inequality gives the asserted result.

We recall that the a priori error for the pressure is obtained by using (5.8) and (5.19). □

Remark 5.2 If instead of (5.16), one uses

$$
\begin{aligned}
&T_1+(H(\boldsymbol{u}_h)-H(R_h\boldsymbol{u}))(\boldsymbol{u}_h-R_h\boldsymbol{u}) \\
&\quad = B(\boldsymbol{u}_h-R_h\boldsymbol{u},\,p-r_hp)+(H(\boldsymbol{u})-H(R_h\boldsymbol{u}))(\boldsymbol{u}_h-R_h\boldsymbol{u}),
\end{aligned}
$$

then we shall have

$$
\begin{aligned}
&|||\boldsymbol{u}-\boldsymbol{u}_h|||_h+\|\boldsymbol{u}_{\boldsymbol{\tau}}-\boldsymbol{u}_{\boldsymbol{\tau},h}\|_{\Gamma}+\|p-p_h\| \\
&\leq c\Big(\sum_{T\in\mathcal{T}_h}\|p-r_hp\|_T^2+h_T^2\|\nabla(p-r_hp)\|_T^2\Big)^{1/2}+c|||R_h\boldsymbol{u}-\boldsymbol{u}|||_h \\
&\quad +c\left(\sum_{e\in\mathcal{E}_h^{\gamma}}h_e^{-1}\|\boldsymbol{u}_{\boldsymbol{\tau}}-(R_h\boldsymbol{u})_{\boldsymbol{\tau}}\|_e^{2(s-1)}\right)^{1/2}.
\end{aligned}
$$

Hence the convergence is not uniform with respect to s.

Remark 5.3 Under the assumption of Theorem 5.1, the solution $(\boldsymbol{u}_h,\,p_h)$ of the DG schemes (see Theorem 4.1) converges strongly to the solution $(\boldsymbol{u},\,p)$ when h tends to

zero. Indeed, for $(\boldsymbol{u}, p) \in H^2(\Omega)^2 \times H^1(\Omega)$, the right hand sides of the two error inequalities obtained tend to zero as h tends to zero. From the error estimate, it is clear that the rate of convergence is linked to the value of s.

Remark 5.4 The error estimates in Theorem 5.1 is dominated by the interpolation error on the slip zone Γ, and it is independent of the parameter s.
If $k = 1$, then

$$|||\boldsymbol{u} - \boldsymbol{u}_h|||_h + \|p - p_h\| \leq ch^{3/4}.$$

If moreover $\boldsymbol{u}_{\boldsymbol{\tau}} \in \boldsymbol{H}^2(\Gamma)$, then

$$|||\boldsymbol{u} - \boldsymbol{u}_h|||_h + \|p - p_h\| \leq c \left(\sum_{e \in \mathcal{E}_h^{\gamma}} \|\boldsymbol{u}_{\boldsymbol{\tau}} - (R_h \boldsymbol{u})_{\boldsymbol{\tau}}\|_e \right)^{1/2} \leq ch.$$

6 Iterative scheme and numerical simulations

The finite element problem (3.6) is nonlinear. Hence iterative/incremental schemes need to be formulated for their effective resolution. It should be noted that since s is in $(1, 2)$, the expression $(|K\boldsymbol{u}_{\boldsymbol{\tau},h}|^{s-2} K\boldsymbol{u}_{\boldsymbol{\tau},h}, K\boldsymbol{v}_{\boldsymbol{\tau},h})_{\Gamma}$ has a poor differentiability. So a numerical solution of (3.6) with Newton's method or conjugate gradient may not converge at all. In the lines that follows, we formulate an iterative method for solving (3.6).

6.1 Iterative scheme for (3.6)

A natural approach is to consider the following algorithm: let $\boldsymbol{u}_h^0$ an element of $\mathbb{V}_h$, for $n \geq 1$ and having $\boldsymbol{u}_h^n$ in $\mathbb{V}_h$, we compute until an adequate stopping condition is satisfied, $(\boldsymbol{u}_h^{n+1}, p_h^{n+1})$ solution of

$$\begin{cases} \text{for all } (\boldsymbol{v}_h, q_h) \in \mathbb{V}_h \times M_h, \\ A(\boldsymbol{u}_h^{n+1}, \boldsymbol{v}_h) + \displaystyle\int_{\Gamma} |K\boldsymbol{u}_{\boldsymbol{\tau},h}^n|^{s-2} K\boldsymbol{u}_{\boldsymbol{\tau},h}^{n+1} \cdot K\boldsymbol{v}_{\boldsymbol{\tau},h} d\sigma + B(\boldsymbol{v}_h, p_h^{n+1}) = F(\boldsymbol{v}_h), \\ B(\boldsymbol{u}_h^{n+1}, q_h) = 0. \end{cases} \quad (6.1)$$

The variational problem (6.1) is linear, and from Babuska–Brezzi's theory for mixed problems (see [5, 22]), $(\boldsymbol{u}_h^{n+1}, p_h^{n+1})$ is well defined. Continuing on the qualitative analysis on (6.1), we now claim that

Lemma 6.1 (see [24]) *The algorithm* (6.1) *is consistent with* (3.6) *in the sense that if* $(\boldsymbol{u}_h^1, p_h^1) = (\boldsymbol{u}_h, p_h)$ *with* $(\boldsymbol{u}_h, p_h)$ *solution of* (3.6)*, then for all* $n \geq 2$, $(\boldsymbol{u}_h^n, p_h^n) = (\boldsymbol{u}_h, p_h)$.

Proof It is done by indiction on n. So, we assume that $(\boldsymbol{u}_h^n, p_h^n) = (\boldsymbol{u}_h, p_h)$, and we will show that $(\boldsymbol{u}_h^{n+1}, p_h^{n+1}) = (\boldsymbol{u}_h, p_h)$.

We use the induction hypothesis, take the difference between (6.1) and (3.6), and obtain

$$\begin{cases} \text{for all } (\boldsymbol{v}_h, q_h) \in \mathbb{V}_h \times M_h, \\ A(\boldsymbol{u}_h^{n+1} - \boldsymbol{u}_h, \boldsymbol{v}_h) + \left(|K\boldsymbol{u}_{\boldsymbol{\tau},h}|^{s-2} K\boldsymbol{u}_{\boldsymbol{\tau},h}^{n+1} - |K\boldsymbol{u}_{\boldsymbol{\tau},h}|^{s-2} K\boldsymbol{u}_{\boldsymbol{\tau},h}, K\boldsymbol{v}_{\boldsymbol{\tau},h} \right)_\Gamma \\ + B(\boldsymbol{v}_h, p_h^{n+1} - p_h) = 0, \\ B(\boldsymbol{u}_h^{n+1} - \boldsymbol{u}_h, q_h) = 0. \end{cases} \tag{6.2}$$

For $(\boldsymbol{v}_h, q_h) = (\boldsymbol{u}_h - \boldsymbol{u}_h^{n+1}, p_h - p_h^{n+1})$ in (6.2), one has

$$A(\boldsymbol{u}_h^{n+1} - \boldsymbol{u}_h, \boldsymbol{u}_h^{n+1} - \boldsymbol{u}_h) + \int_\Gamma |K\boldsymbol{u}_{\boldsymbol{\tau},h}|^{s-2} \left| K\boldsymbol{u}_{\boldsymbol{\tau},h}^{n+1} - K\boldsymbol{u}_{\boldsymbol{\tau},h} \right|^2 d\sigma = 0$$

from which we deduce that (since $A(\cdot,\cdot)$ is coercive) $\boldsymbol{u}_h^{n+1} = \boldsymbol{u}_h$.
Equations (6.2) is then reduced to

$$\text{for all } \boldsymbol{v}_h \in \mathbb{V}_h, \quad B(\boldsymbol{v}_h, p_h^{n+1} - p_h) = 0. \tag{6.3}$$

The inf-sup condition (4.5) together with (6.3) gives $p_h^{n+1} = p_h$. □

In order to justify why we use the iterative scheme (6.1) (implemented in paragraph 6.2) to compute the solution of (3.6), we shall prove a convergence result. For that purpose, we first claim that

Lemma 6.2 *Let $(\boldsymbol{u}_h^{n+1}, p_h^{n+1})$ be the solution of the algorithm (6.1). Then there exists a constant c independent of h and n such that*

$$\|\nabla \boldsymbol{u}_h^{n+1}\| + \|p_h^{n+1}\| \leq c.$$

Proof We take $\boldsymbol{v}_h = \boldsymbol{u}_h^{n+1}$ in (6.1) and obtain

$$A(\boldsymbol{u}_h^{n+1}, \boldsymbol{u}_h^{n+1}) + \int_\Gamma |K\boldsymbol{u}_{\boldsymbol{\tau},h}^n|^{s-2} \left| K\boldsymbol{u}_{\boldsymbol{\tau},h}^{n+1} \right|^2 d\sigma = F(\boldsymbol{u}_h^{n+1}) \leq c(\boldsymbol{f}, g) \|D\boldsymbol{u}_h^{n+1}\|$$

which implies that

$$\|\nabla \boldsymbol{u}_h^{n+1}\| \leq c |||\boldsymbol{u}_h^{n+1}|||_h \leq c(\boldsymbol{f}, g).$$

From the inf-sup condition (see (4.5)), we obtain that

$$\|p_h^{n+1}\| \leq c(\boldsymbol{f}, g).$$

□

We have the following abstract convergence result

Theorem 6.1 *Assume that* Γ *is of class* $\mathcal{C}^{1,1}$. *Let* $(\boldsymbol{u}_h^{n+1}, p_h^{n+1}) \in \mathbb{V}_h \times M_h$ *be the solution of* (6.1), *and* $(\boldsymbol{u}_h, p_h) \in \mathbb{V}_h \times M_h$ *the solution of* (3.6). *Then*

$$\lim_{n\to\infty} \boldsymbol{u}_h^n = \boldsymbol{u}_h \text{ weakly in } \mathbb{V}.$$

Proof By virtue of the bound obtained in Lemma 6.2, there is a subsequence, still denoted by $\{\boldsymbol{u}_h^n\}_n$ such that

$$\lim_{n\to\infty} \boldsymbol{u}_h^n = \widetilde{\boldsymbol{u}}_h \quad \text{weakly in } \ H^1(\Omega)^2. \tag{6.4}$$

Clearly, we need to show that $\widetilde{\boldsymbol{u}}_h = \boldsymbol{u}_h$, this is to say that

$$\begin{cases} \text{for all } \boldsymbol{v}_h \in \mathcal{Z}_h, \\ A(\widetilde{\boldsymbol{u}}_h, \boldsymbol{v}_h) + \left(|K\widetilde{\boldsymbol{u}}_{\boldsymbol{\tau},h}|^{s-2} K\widetilde{\boldsymbol{u}}_{\boldsymbol{\tau},h}\ ,\ K\boldsymbol{v}_{\boldsymbol{\tau},h}\right)_\Gamma = F(\boldsymbol{v}_h). \end{cases} \tag{6.5}$$

Actually, since $\mathcal{Z}_h$ is closed, it follows from (6.4) that $\widetilde{\boldsymbol{u}}_h \in \mathcal{Z}_h$. Owing to the compactness of the imbedding of $H^1(\Omega)$ into $L^4(\Omega)$, there exists a subsequence, still denoted by $\{\boldsymbol{u}_h^n\}_n$, which converges weakly to $\widetilde{\boldsymbol{u}}_h \in H^1(\Omega)^2$ and strongly in $L^4(\Omega)^2$. For $\boldsymbol{v}_h \in \mathcal{Z}_h$, passing to the limit on n in (6.1) is direct for the linear term because one only need weak convergence (6.4). Next, for the term on Γ, we deduce from the weak convergence of $\boldsymbol{u}_h^n$ on $H^1(\Omega)^2$, that

$$\boldsymbol{u}_h^n \to \widetilde{\boldsymbol{u}}_h \quad \text{strongly in } \ L^2(\Omega)^2,$$

and the trace from $H^{1/2}(\Gamma)$ into $L^2(\Gamma)$ is compact provided that Γ is at least $\mathcal{C}^{1,1}$. Hence

$$\boldsymbol{u}_h^n|_\Gamma \to \widetilde{\boldsymbol{u}}_{\boldsymbol{\tau},h}|_\Gamma \quad \text{weakly in } L^2(\Gamma)^2.$$

Now from the fact that the mapping $\boldsymbol{v} \to \mathcal{B}\boldsymbol{v} = |K\boldsymbol{v}_{\boldsymbol{\tau}}|^{s-2} K\boldsymbol{v}_{\boldsymbol{\tau}}$ is monotone, and hemi-continuous, and the strong convergence $\boldsymbol{u}_h^n|_\Gamma$, we deduce that (see [38, Chap 2])

$$\begin{aligned} \lim_n \left(|K\boldsymbol{u}_{\boldsymbol{\tau},h}^n|^{s-2} K\boldsymbol{u}_{\boldsymbol{\tau},h}^{n+1}\ ,\ K\boldsymbol{v}_{\boldsymbol{\tau},h}\right)_\Gamma &= \lim_n \left(|K\boldsymbol{u}_{\boldsymbol{\tau},h}^n|^{s-2} K\boldsymbol{u}_{\boldsymbol{\tau},h}^n\ ,\ K\boldsymbol{v}_{\boldsymbol{\tau},h}\right)_\Gamma \\ &= \left(|K\widetilde{\boldsymbol{u}}_{\boldsymbol{\tau},h}|^{s-2} K\widetilde{\boldsymbol{u}}_{\boldsymbol{\tau},h}\ ,\ K\boldsymbol{v}_{\boldsymbol{\tau},h}\right)_\Gamma. \end{aligned}$$

Hence, $\widetilde{\boldsymbol{u}}_h$ satisfy (6.5), and $\widetilde{\boldsymbol{u}}_h = \boldsymbol{u}_h$ since the solution of (6.5) is unique. Then the entire sequence converges weakly to $\boldsymbol{u}_h$. □

6.2 Simulations

In this section, we study the numerical behavior of the algorithm (6.1). For that purpose, we evaluate the performances of the algorithm (6.1) by solving two problems in 2d. First, we assess the convergence properties of the numerical method by using the standard mesh refinement strategy. The second example is concerned with the Lid-Driven cavity, a well studied problem in computational mechanics (see for instance [27]). All the numerical simulations showed in this section are performed with FreeFem++ [28] by taking $\boldsymbol{u}_h^0 = \mathbf{0}$.

The bilinear forms are defined in (3.5), and the resulting system of equations to be solved are called (with obvious identification); *SIPG*, *NIPG* and *IIPG*. The stabilization parameter for these schemes are denoted respectively by α_{SIPG}, α_{NIPG} and α_{IIPG}. These constants are positive and as indicated by the coercivity, α_{SIPG} should be bounded below by sufficiently large positive real number. We take the tensors

$$K_1 = I \quad \text{and} \quad K_2 = \begin{bmatrix} 5 & -1 \\ -1 & 4 \end{bmatrix}.$$

The couple velocity-pressure is approximated by $\mathcal{P}_1(T)^2 \times \mathcal{P}_0(T)$ for all $T \in \mathcal{T}_h$, furthermore, for the iterative scheme (6.1), we use the following stopping criterion

$$\frac{|||\boldsymbol{u}_h^{n+1} - \boldsymbol{u}_h^n|||_h + ||\boldsymbol{u}_{\boldsymbol{\tau},h}^{n+1} - \boldsymbol{u}_{\boldsymbol{\tau},h}^n||_\Gamma + ||p_h^{n+1} - p_h^n||}{|||\boldsymbol{u}_h^{n+1}|||_h + ||\boldsymbol{u}_{\boldsymbol{\tau},h}^{n+1}||_\Gamma + ||p_h^{n+1}||} \leq 10^{-5}.$$

6.2.1 Stokes flow in a square: rate of convergence

The flow domain is $\Omega = (0, 1)^2$, and each side is divided into N segments of equal length. Thus the corresponding mesh contains $2N^2$ elements. We set $\nu = 1$, $K = K_1$ and $\boldsymbol{f} = (x^2 + y^2, 1)^T$. The anisotropic slip boundary conditions (1.4) and (1.6), are considered on $\Gamma = \{(x, y)|\ x = 1 \text{ or } y = 1\} = \overline{\Gamma_2 \cup \Gamma_3}$, and the homogeneous Dirichlet boundary condition $\boldsymbol{u} = \mathbf{0}$ is taken on $S = \partial\Omega \backslash \Gamma = \overline{\Gamma_1 \cup \Gamma_4}$.
First we will show the dependency of the convergence and the precision of the schemes *SIPG*, *NIPG* and *IIPG* respectively with respect to the parameters α_{SIPG}, α_{NIPG} and α_{IIPG} for $s = 3/2$. Since we do not have the exact solution $(\boldsymbol{u}, p)$ for this problem, we shall approximate it by computing the finite element solution with Taylor-Hood's elements associated to (2.2). The corresponding solution will be considered as the reference solution say, $(\boldsymbol{u}_{ref}, p_{ref})$ computed for $N = 100$. We test the algorithm (6.1) corresponding to *SIPG*, *NIPG* and *IIPG* for $N = 40$ and for α_{IIPG}, α_{NIPG} and α_{SIPG} in [0, 200]. Figure 1 (with a zoom on the right) shows the following error

$$E_a = \frac{|||\boldsymbol{u}_{ref} - \boldsymbol{u}_h|||_h + ||\boldsymbol{u}_{\tau,ref} - \boldsymbol{u}_{\tau,h}||_\Gamma + ||p_{ref} - p_h||}{|||\boldsymbol{u}_{ref}|||_h + ||\boldsymbol{u}_{\boldsymbol{\tau},ref}||_\Gamma + ||p_{ref}||} \tag{6.6}$$

where $\boldsymbol{u}_h$ is computed by using the iterative schemes *SIPG*, *NIPG* and *IIPG*. We can deduce that the better results (with $E_a \leq 0.05$) correspond to α are α_{IIPG} in [6, 74],

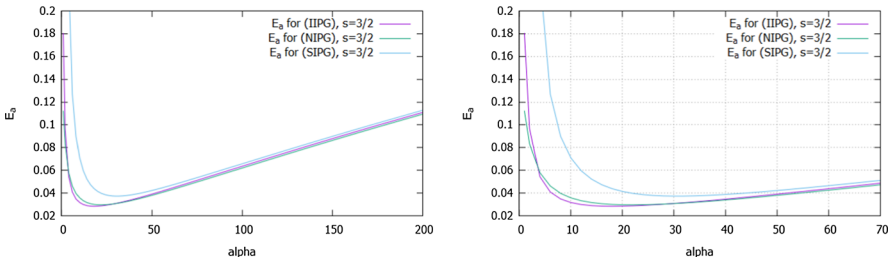

Fig. 1 E_α associated to the iterative schemes *SIPG*, *NIPG* and *IIPG* for $\alpha \in [1, 200]$ (zoom on the right)

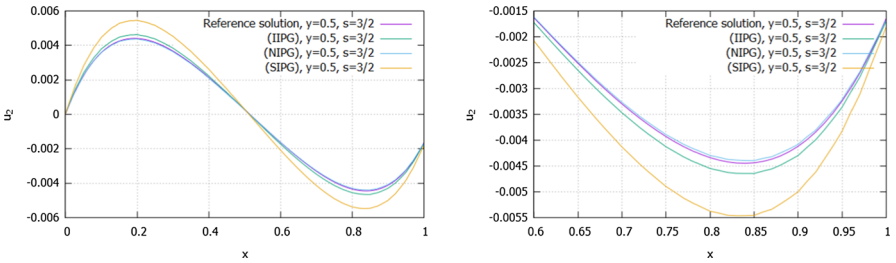

Fig. 2 Second component of the velocity, u_2 on the line $y = 0.5$ for the reference solution and those obtained with *SIGP*, *NIPG* and *IIPG* for $\alpha = 20$ (zoom on the right)

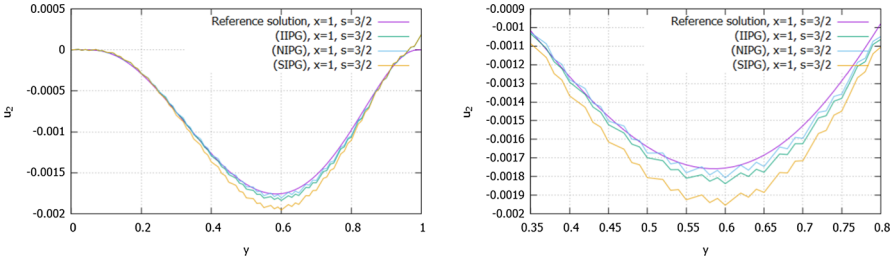

Fig. 3 Second component of the velocity, u_2 on the line $x = 1$ for the reference solution and those obtained with *SIPG*, *NIPG* and *IIPG* for $\alpha = 20$ (zoom on the right)

α_{NIPG} in [6, 74] and α_{SIPG} in [16, 68]. In all these situations, the algorithm converges after 10–12 iterations. Similar numerical results are obtained for $s = 4/3$ and $s = 7/4$. In the following, we take $\alpha_{IIPG} = \alpha_{NIPG} = \alpha_{SIPG} = 20$.

Figure 2 (resp Fig. 3) shows (with a zoom on the right) comparisons of the second component of the velocity (say u_2) between the reference solution and those obtained with the iterative schemes *SIPG*, *NIPG* and *IIPG* on the horizontal line $y = 0.5$ (resp. $x = 1$). We clearly see that the schemes *NIPG* and *IIPG* give the better results, while the results obtained with the scheme *SIPG* are less precise.

Let us now check the *a priori* error estimates corresponding to the schemes *SIGP*, *NIPG* and *IIPG*. We take $s = 4/3$ and $s = 7/4$, and we are interested in computing the rate of convergence of the numerical solution $(\boldsymbol{u}_h, p_h)$. We recall that (Theorem 5.1)

Table 1 The slopes of the schemes *SIPG* and *IIPG* with respect to α

Value of α	15	20	30	50	100
Slope for *SIPG*	–	–	0.74	0.64	0.40
Slope for *IIPG*	0.95	0.93	0.85	0.68	0.41

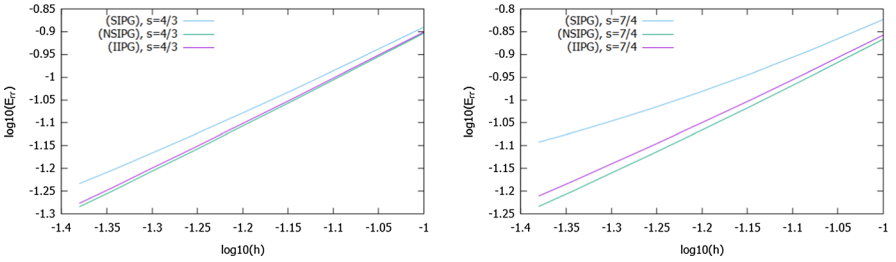

Fig. 4 Error estimate with respect to the mesh step h in logarithmic scale for $s = 4/3$ (left) and $s = 7/4$ (right), and associated to the schemes *SIPG*, *NIPG* and *IIPG*

$$|||\boldsymbol{u} - \boldsymbol{u}_h|||_h + \|p - p_h\| \leq ch \quad \text{if } (\boldsymbol{u}, p) \in H^2(\Omega)^2 \times H^1(\Omega), \boldsymbol{u_\tau} \in H^2(\Gamma)^2. \tag{6.7}$$

We denote by E_{rr} the same expression of E_a in (6.6) but with $\alpha = 20$ for each scheme *IIPG*, *NIPG* and *SIPG*. To get the *a priori* error estimate corresponding to our schemes, we compute the numerical solution $(\boldsymbol{u}_h, p_h)$ for $N = 10, 12, 14, \ldots, 24$. Figure 4 shows the graphs of the relative error E_{rr} with respect to $h = \dfrac{1}{N}$ in logarithmic scale. These lines have the slopes 0.99, 0.99, 0.95 for $s = 4/3$ and 0.94, 0.97, 0.71 for $s = 7/4$, respectively for *IIPG*, *NIPG* and *SIPG*. We can partially deduce that the numerical slopes associated to the schemes *IIPG* and *NIPG* are in agreement with (6.7), while the slope associated to the scheme *SIPG* is sub-optimal. The bad behavior observed for *SIPG* can be explained by the fact that the bilinear form $A^{SIPG}(\cdot, \cdot)$ is conditionally elliptic (see Lemma 4.3). Next, Fig. 5 (resp. Fig. 6) show E_{rr} with respect to h for each value of α in logarithmic scale computed by using the scheme *SIPG* (resp. the scheme *IIPG*). We note that for the values of α taken, the curves are straight lines when $\alpha \geq 30$ for the scheme *SIPG*, and when $\alpha \geq 15$ for the scheme *IIPG*. Table 1 shows the variation of the slopes of the lines corresponding to E_{rr} computed with the schemes *NIPG* and *IIPG* with respect to α. We note that the convergence is optimal for the scheme *IIPG* (since the slope is almost one for some values of α), while in Fig. 1 we observe a degradation of the slope for all the schemes when the stabilisation parameter is big.

6.3 Lid driven cavity flow

In this paragraph, we consider the numerical results via the algorithm (6.1) of the Lid Driven cavity Stokes flow with power law slip boundary condition. The fluid is confined in the xy-plane with $(x, y) \in (0, 1)^2$ and the boundary condition for the

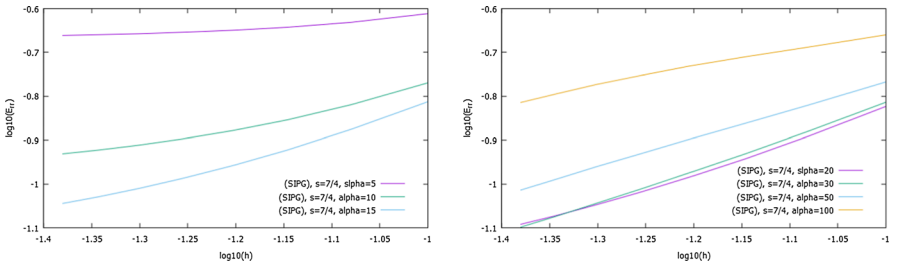

Fig. 5 rate of convergence with the scheme *SIPG* for $s = 7/4$ and for $\alpha = 5, 10, 15$ (left) and $\alpha = 15, 20, 30, 50, 100$ (right)

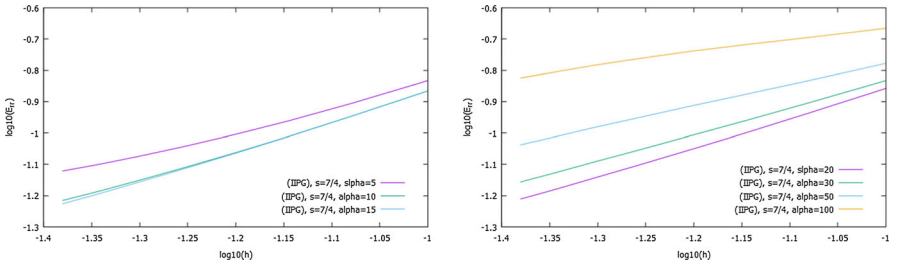

Fig. 6 rate of convergence with the scheme *IIPG* for $s = 7/4$ and for $\alpha = 5, 10, 15$ (left) and $\alpha = 15, 20, 30, 50, 100$ (right)

velocity field given by

$$\boldsymbol{u} = \begin{cases} (16\,x^2(x-1)^2, 0)^T & \text{on } \; y = 1, \;\; 0 < x < 1, \\ (0,0)^T & \text{elsewhere.} \end{cases}$$

Thus one has a smooth start of the flow, and the lid velocity attains its maximum, $\boldsymbol{u} = (1,0)^T$, at the center $x = 1/2$. This boundary condition has the effect of avoiding local singularities at the top-right and top-left corners as it ensures both the velocity and velocity gradient vanish at the corners. Furthermore, we consider the isotropic slip boundary condition on the other parts of the boundary. In all the numerical results considered in this section, we set $N = 100$, $K = K_2$, $\boldsymbol{f} = \boldsymbol{0}$ and $\nu = 1$. Based on the results showed in the previous section, we will show in this case the numerical results corresponding to the schemes *IIPG* and *NIPG* and we will omit the those of the scheme *SIPG*.

Figure 7 shows repartition of the velocity associated to the schemes *IIPG* and *NIPG* for $s = 3/2$, $K = K_2$ and $\alpha = 20$. These figures are closed and one can deduce that the schemes *IIPG* and *SIPG* shall give similar results.

Next, Fig. 8 shows comparisons of the first and second components of the velocity on the horizontal line $y = 0.5$ between *IIPG* and *NIPG* for $K = K_2$. Here also *IIPG* and *SIPG* gives close results.

In order to test the dependency of the convergence with the Reynolds number, Fig. 9 shows for $Re = 2000$ the repartition of the velocity in the domain for $\alpha = 20$.

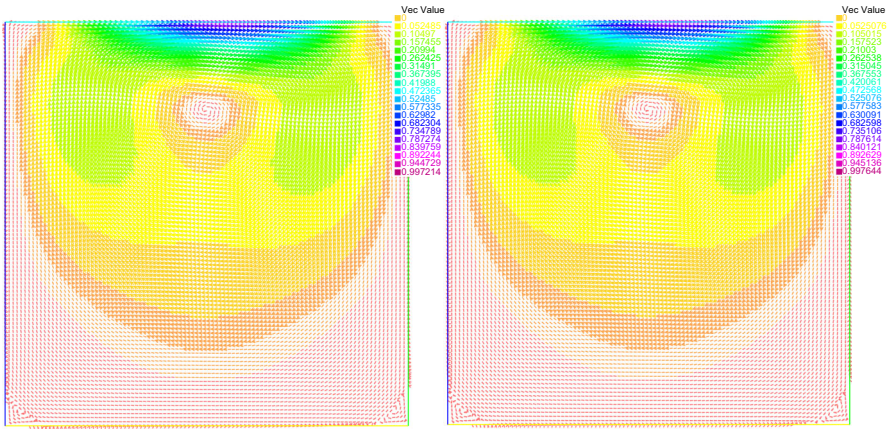

Fig. 7 Distribution of the velocity for the schemes *IIPG* on the left and *NIPG* on the right with $K = K_2$, $\alpha = 20$ $N = 100$ and $s = 3/2$

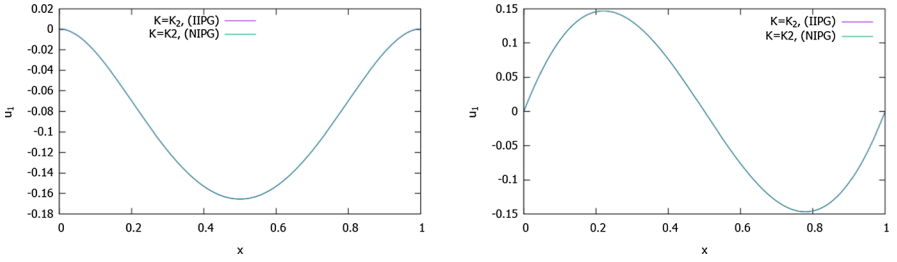

Fig. 8 First and second components of the velocity on the line $y = 0.5$ for $K = K_2$

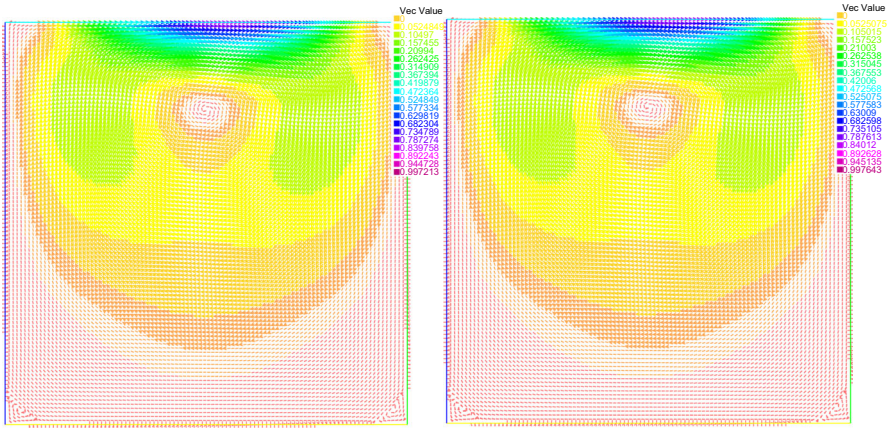

Fig. 9 Distribution of the velocity for $Re = 2000$ using *IIPG* on the left and *NIPG* on the right for $\alpha = 20$, $K = K_2$

7 Conclusion

Three DG schemes are formulated and analysed to study the Stokes equations under power law slip boundary condition. The DG approximations lead to a nonlinear set of equations which are analyzed by exploiting the rich structure of the resulting variational formulation. Existence of solutions, a priori error estimates and convergence of DG solutions are thoroughly studied. For the effective computation of the DG solutions, we formulate and analyze a fixed approach. To be more precise, we show the convergence of the fixed point strategy by making use of the weak convergence method. Finally, two numerical experiments are shown: the first one illustrates the convergence properties of the method, while the second one shows the applicability of the method on a benchmark test. From the simulations (considering the data used), it appears that the *NIPG* and *IIPG* schemes are the best performing numerical schemes.
The current methodology should be further developed, in particular by (i) devising an adapted discretization strategy; (ii) considering the case of a curved boundary; (iii) extending the present analysis to non-linear Stokes equations (or Generalized non-Newtonian models); (iv) considering the present work with singular force (Dirac measure).

Acknowledgements The authors thank the referee for his/her valuable remarks and comments.

Funding Not applicable.

Data availability Not applicable

Declarations

Conflict of interest The authors declare no conflict of interest

Informed consent Not applicable.

References

1. Arnold, D.N.: An interior penalty finite element method with discontinuous elements. Siam J. Numer. Anal. **19**(4), 642–760 (1982)
2. Arnold, D.N., Brezzi, F., Cockburn, B., Marini, L.D.: Unified analyis of discontious Galerkin methods for elliptic problems. SIAM J. Numer. Anal. **39**, 1749–1779 (2002)
3. Baranger, J., Najib, K.: Analyse numerique des ecoulements quasi-Newtoniens dont la viscosite obeit a la loi puissance ou la loi de carreau. Numer. Math. **58**, 35–49 (1990)
4. Bodart, O., Chorfi, A., Koko, J.: A fictitious domain decomposition method for a nonlinear bonded structure. Math. Comput. Simul. **189**(7), 114–125 (2021)
5. Boffi, D., Brezzi, B., Fortin, M.: Mixed Finite Element Methods and Applications. Springer Series in Computational Mathematics, Springer, Berlin (2013)
6. Bresch, D., Koko, J.: An optimization-based domain decomposition method for nonlinear wall laws in coupled systems. Math. Models Methods Appl. Sci. **14**(7), 1085–1101 (2004)
7. Brenner, S.C.: Korn's inequalities for piecewise H^1 vector fields. Math. Comput. **73**, 1067–1087 (2004)
8. Brezis, H.: Functional Analysis, Sobolev Spaces and partial differential equations. Springer, Berlin (2010)
9. Busse, A., Sandham, N.D.: Influence of an anisotropic slip-length boundary condition on turbulent channel flow. Phys. Fluids. **24**, 055111 (2012). https://doi.org/10.1063/1.4719780

10. Charrault, E., Lee, T., Neto, C.: Interfacial slip on rough, patterned and soft surfaces: a review of experiments and simulations. Adv. Colloid Interface Sci. **210**, 21–38 (2014)
11. Cooper, A.J., Harris, J.H., Garrett, S., Jözkan, M., Thomas, P.J.: The effect of anisotropic and isotropic roughness on the convective stability of the rotating disk boundary layer. Phys. Fluids. **27**, 014107 (2015). https://doi.org/10.1063/1.4906091
12. Crouzeix, M., Raviart, P.A.: Conforming and nonconforming finite element methods for solving the stationary Stokes equations. *RAIRO.*, Ser. Rouge. 33–75 (1973)
13. Crouzeix, M., Falk, R.S.: Non conforming finite elements for the Stokes problem. Math. Comput. **52**, 437–456 (1989)
14. Dawson, C., Sun, S., Wheeler, M.F.: Compatible algorithms for coupled flow and transport. Comput. Methods Appl. Mech. Eng. **193**, 2565–2580 (2004)
15. Dione, I., Tibirna, C., Urquiza, J.M.: Stokes equations with penalized slip boundary conditions. Int. J. Comput. Fluid Dyn. **27**, 283–296 (2013)
16. Dione, I., Urquiza, J.M.: Penalty finite element approximation of Stokes equations with slip boundary conditions. Numer. Math. **129**, 587–610 (2015)
17. Djoko, J.K., Koko, J., Mbehou, M., Sayah, T.: Stokes and Navier–Stokes equations under power law slip boundary condition: numerical analysis. Comput. Math. Appl. **128**, 198–213 (2022)
18. Evans, L.C., Gariepy, R.F.: Measure Theory and Fine Property of Functions. CRC Press, Boca Raton (1992)
19. Fortin, M., Souli, M.: A non-conforming piecewise quadratic finite element on triangles. Int. J. Numer. Methods Eng. **19**, 505–520 (1983)
20. Fouchet-Incaux, J.: Artificial boundaries and formulations for the incompressible Navier–Stokes equations: applications to air and blood flows. SeMA J. **64**, 1–40 (2014)
21. Geymonat, G., Krasucki, F., Marini, D., Vidrascu, M.: A domain decomposition method for bonded structures. Math. Models Methods Appl. Sci. **8**(8), 1387–1402 (1998)
22. Girault, V., Raviart, P.A.: Finite Element Methods for Navier–Stokes Equations: Theory and Algorithms. Springer, Berlin (1986)
23. Girault, V., Riviere, B., Wheeler, M.F.: A discontinuous Galerkin method with non overlapping domain decomposition for the Stokes and Navier–Stokes problems. Math. Comput. **74**, 53–84 (2004)
24. Girault, V., Wheeler, M.F.: Numerical discretization of a Darcy–Forchheimer model. Numer. Math. **110**, 161–198 (2008)
25. Glowinski, R.: Finite element methods for incompressible viscous flow. In: Ciarlet, P.G., Lions, J.L. (eds.) Handbook of Numerical Analysis, vol. IX, p. 176. North Holland, Amsterdam (2003)
26. Glowinski, R., Morrocco, A.: Sur l approximation par elements finis d ordre un et la resolution par penalisation-dualite d une classe de problemes de Dirirchlet nonlineaires. *Rairo.*, serie rouge- Analyse numerique, **9**, 41–76 (1975)
27. Glowinski, R., Guidoboni, G., Pan, T.W.: Wall-driven incompressible viscous flow in a two-dimensional semi-circular cavity. J. Comput. Phys. **216**, 76–91 (2006)
28. Hecht, F.: New development in FreeFem++. J. Numer. Math. **20**, 251–266 (2012)
29. Jao, Hsiang-Chin., Chang, Kuo-Ming., Chu, Li-Ming., Li, Wang-Long.: A lubrication theory for anisotropic slips and flow rheology. Tribol. Trans. **59**(2), 252–266 (2016)
30. Kaya, S., Riviere, B.: A discontinuous subgrid eddy viscosity method for the time dependent Navier–Stokes equations. SIAM J. Numer. Anal. **43**, 1572–1595 (2005)
31. Koko, J.: An optimization based domain decomposition method for a bonded structure. Math. Models Methods Appl. Sci. **12**(6), 857–870 (2002)
32. Koko, J.: Convergence analysis of optimization-based domain decomposition methods for a bonded structure. Appl. Numer. Math. **58**, 69–87 (2008)
33. Koko, J.: Lagrangian multiplier based domain decomposition methods for a nonlinear sedimentary basin problem. Comput. Geosci. **11**, 307–317 (2007)
34. Koko, J.: Uzawa conjugate gradient domain decomposition methods for coupled Stokes flows. J. Sci. Comput. **26**(2), 195–216 (2006)
35. Jingang, Lu., Jang, Hye Kyeong, Lee, Sang Bok, Hwang, Wook Ryol: Characterization on the anisotropic slip for flows over unidirectional fibrous porous media for advanced composites manufacturing. Compos. A Appl. Sci. Manuf. **100**, 9–19 (2017)
36. Le Roux, C.: Flows of incompressible viscous liquids with anisotropic wall slip. J. Math. Anal. Appl. **465**, 723–730 (2018)

37. Le Roux, C.: On the Navier–Stokes equations with anisotrpic wall slip conditions. Appl. Math. (2022). https://doi.org/10.21136/AM.2021.0079-21
38. Lions, J.L.: Quelques Méthodes de Résolution des Problèmes aux Limites Non Linéaires. Dunod, Paris (1969)
39. Alam Khan, Najeeb, Sohail, Ayesha, Sultan, Faqiha: Effect of anisotropic slip and magnetic field on the flow and heat transfer of Eyring Powell fluid over an inifinite rotating disk. Int. J. Fluid Mech. Res. **44**(3), 257–273 (2017)
40. Riviere, B., Wheeler, M.F., Girault, V.: Improved energy estimates for interior penalty constrained and discontinuous Galerkin method for elliptic problems. Part 1. Comput. Geosci. **3**(3–4), 337–360 (1999)
41. Sandri, D.N.: Sur l approximation des ecoulements numeriques quasi-Newtoniens dont la viscosite obeit a la loi de puissance ou de Carreau. M2AN **27**, 131–155 (1993)
42. Raviart, P.A., Thomas, J.M.: A mixed finite element method for second order elliptic problems. In: Mathematical Aspects of Finite Element Methods. Lecture Notes in Mathematics, vol. 606. Springer, Berlin (1975)
43. Schotzau, D., Schwab, C., Toselli, A.: Mixed HP-DGFEM for incompressible flows. SIAM J. Numer. Anal. **40**, 2171–2194 (2002)
44. Scott, L.R., Zhang, S.: Finite element interpolation of non-smooth functions satisfying boundary conditions. Math. Comput. **54**, 483–493 (1990)
45. Verfurth, R.: Finite element approximation of incompressible Navier–Stokes equations with slip boundary condition II. Numer. Math. **50**, 697–721 (1987)
46. Verfurth, R.: Finite element approximation of incompressible Navier–Stokes equations with slip boundary condition II. Numer. Math. **59**, 615–636 (1991)
47. Zhou, G., Oikawav, I., Kashiwabara, T.: The Crouzeix–Raviart element for the Stokes equations with the slip boundary condition on a curved boundary. J. Comput. Appl. Math. **383**, 113–123 (2020)
48. Zhou, G., Oikawav, I., Kashiwabara, T.: Penalty method with Crouzeix–Raviart approximation for the Stokes equations under slip boundary condition. ESAIM: M2AN **53**(3), 869–891 (2019)

Publisher's Note Springer Nature remains neutral with regard to jurisdictional claims in published maps and institutional affiliations.

Springer Nature or its licensor (e.g. a society or other partner) holds exclusive rights to this article under a publishing agreement with the author(s) or other rightsholder(s); author self-archiving of the accepted manuscript version of this article is solely governed by the terms of such publishing agreement and applicable law.